of this finding was underscored by the fact that disease-causing missense mutations in PHD1 abolished its E3 ligase activity (10).

One important aspect of AIRE, in the context of autoimmunity, is its limited tissue expression in medullary thymic epithelial cells (mTEC) and cells of the monocyte-dendritic cell lineage of the thymus (13, 14). Both cell types are considered to play major roles in the establishment of self-tolerance by eliminating autoreactive T cells (negative selection) (1, 15) and/or by producing immunoregulatory T cells (Tregs), which prevent $CD4^+$ T cell-mediated organ-specific autoimmune diseases (16, 17). For this purpose, thymic epithelial cells (TECs) have been postulated to express a set of self-Ags encompassing all of the self-Ags expressed by parenchymal organs. Supporting this hypothesis, analysis of gene expression in the thymic stroma has demonstrated that mTECs are a specialized cell type in which promiscuous expression of a broad range of peripheral tissue-specific genes is an autonomous property (18). Aire in TECs has been suggested to regulate this promiscuous gene expression (19).

Fundamental roles of Aire in the elimination of autoreactive T cells in vivo have been demonstrated by the use of a TCR-transgenic mouse system (20). Mice expressing hen egg lysozyme (HEL) in pancreatic β cells driven by the rat insulin promoter were crossed with mice expressing TCR specific for HEL, and the fate of HEL-specific T cells was monitored in either the presence or absence of Aire. Remarkably, Aire-deficient TCR-transgenic mice showed almost complete failure to delete the autoreactive (i.e., HEL specific) T cells in the thymus (20). Because Aire-deficient mTEC showed a reduction in transcription of a group of genes encoding peripheral Ags analyzed by the gene-chip technique (19), it has been hypothesized that pathogenic autoreactive T cells could not be eliminated efficiently due to the reduced expression of corresponding target Ags in the Aire-deficient thymus (20). However, as this transgenic study did not demonstrate the effect of Aire loss on the thymic expression of HEL, there is still a lack of experimental evidence to connect the postulated roles of Aire in the transcriptional regulation of tissue-specific Ag expression with efficient elimination of autoreactive T cells. Thus, beyond transcriptional control of self-Ags in the thymus, other mechanisms of AIRE-dependent tolerance remain to be investigated. Furthermore, the effect of Aire deficiency on the production and/or function of Tregs has not yet been fully documented (19–21). Finally, the factors contributing to the complexity of the APECED phenotype (i.e., involvement of various target organs among patients) are unknown. Although intrafamilial variation in the clinical pictures suggests that factors other than the specific *AIRE* mutations might be involved in the disease process (22), this hypothesis cannot be easily proven in human subjects. To approach these issues, we have generated Aire-deficient mice by gene targeting. Identification of a target Ag associated with the tissue destruction caused by Aire deficiency together with strain-dependent target-organ specificity of the autoimmune disease has suggested unique properties of AIRE in the establishment and maintenance of self-tolerance.

Materials and Methods

Mice

Aire-deficient mice were generated by gene targeting. Briefly, the targeting vector was constructed by replacing the genomic *Aire* locus starting from exon 5 to exon 12 with the neomycin resistance gene (neo^r). The targeting vector was introduced into TT2 embryonic stem cells ($H\text{-}2^{b/k}$) (23), and the homologous recombinant clones were first identified by PCR and confirmed by Southern blot analysis. After the targeted cells had been injected into ICR 8 cell embryos (CLEA Japan), the resulting chimeric male mice were mated with C57BL/6 females to establish the germline transmission. C57BL/6 mice, BALB/c mice, and BALB/cA Jcl-ν mice were purchased from CLEA Japan. The mice were maintained under pathogen-free conditions and handled in accordance with the Guidelines for Animal Experimentation of Tokushima University School of Medicine. The experiments were initiated when the mice were 8–12 wk of age.

Pathology

Formalin-fixed tissue sections were subjected to H&E staining, and two pathologists independently evaluated the histology without being informed of the condition of each individual mouse. Histological changes were scored as 0 (no change), 1 (mild lymphoid cell infiltration), or 2 (marked lymphoid cell infiltration).

Measurement of tear secretion

Measurement of tear secretion was performed as previously described (24, 25). Briefly, anesthetized mice were injected i.p. with 100 μl of pilocarpine hydrochloride (1 mg/ml) to stimulate tear production. Secreted tears were absorbed every 5 min with a cotton thread treated with a pH indicator phenol red (ZONE-QUICK; Menicon), and the length of the red portion of the thread was measured each time. Total length of the red portion of the thread during the first 20 min after pilocarpine injection was normalized by body weight.

ELISA and Western blot analysis

Various forms of recombinant α-fodrin were expressed with pGEX-4Ts plasmids (26). Western blot analysis and ELISA for the detection of auto-Abs against various forms of recombinant α-fodrin were performed with anti-mouse IgG Ab (Vector Laboratories), as described previously (25, 27–31). For the ELISA, absorbance values greater than the mean $\pm$ 3 SD in wild-type sera were considered positive. Western blot analysis of α-fodrin expression from the proteins extracted from the thymus and lacrimal glands was performed with mouse anti-α-fodrin mAb (Affiniti) and rabbit anti-AFN-A polyclonal Ab (25, 27–31).

Autoreactive responses against α-fodrin

For in vitro stimulation with α-fodrin, total splenocytes were stimulated with 10 μg/ml recombinant α-fodrin. For the last 8 h of the 32-h culture period, the cells were pulsed with [^{3}H]thymidine, and ^{3}H incorporation was determined as described previously (25).

Thymic stroma preparation

Thymic stroma was prepared as described previously with slight modification (32). Briefly, thymic lobes were isolated from three mice for each group and cut into small pieces. The fragments were gently rotated in RPMI 1640 medium (Invitrogen) supplemented with 10% heat-inactivated FCS (Invitrogen), 20 mM HEPES, 100 U/ml penicillin, 100 μg/ml streptomycin, and 50 μM 2-ME, hereafter referred to as R10, at 4°C for 30 min, and dispersed further with pipetting to remove the majority of thymocytes. The resulting thymic fragments were digested with 0.15 mg/ml collagenase IV (Sigma-Aldrich) and 10 U/ml DNase I (Roche Molecular Biochemicals) in RPMI 1640 at 37°C for 15 min. The supernatants that contained dissociated TECs were saved, whereas the remaining thymic fragments were further digested with collagenase IV and DNase I. This step was repeated twice, and the remaining thymic fragments were digested with collagenase IV, DNase I, and 0.1 mg/ml dispase I (Roche Applied Science) at 37°C for 30 min. The supernatants from this digest were combined with the supernatants from the collagenase digests, and the mixture was centrifuged for 5 min at 450 $\times$ *g*. The cells were suspended in PBS containing 5 mM EDTA and 0.5% FCS and kept on ice for 10 min. $CD45^-$ thymic stromal cells were then purified by depleting $CD45^+$ cells with MACS CD45 microbeads (Miltenyi Biotec) according to the manufacturer's instructions. The resulting preparations contained ~60% Ep-CAM^+ cells and <10% thymocytes (i.e., CD4/CD8 single-positive and CD4/CD8 double-positive cells), as determined by flow cytometric analysis.

RT-PCR

RNA was extracted from thymic stromal cells with High Pure RNA isolation kit (Roche Applied Science) and made into cDNA with cDNA Cycle kit (Invitrogen) according to the manufacturer's instructions. The following primer pairs for the *α-fodrin* gene were used: 5′-GCTTCAAGGAG CTCTCTACC-3′ and 5′-GCAGTTTGATTCCTTTCTCC-3′ (encompassing *α-fodrin* exons 1–3; accession no. XM_355324), 5′-CCAGCAGCAA CAATTTAATC-3′ and 5′-AGCAGATTCTGGACTCCAAT-3′ (encompassing the *α2-spectrin* exons 2–4; accession no. XM_207079), and 5′-GTG CAGAAATCAGCTGAGAA-3′ and 5′-GCTTGTGTTTCTTCCTCAGA-3′ (encompassing the *α2-spectrin* exons 24–27). PCR was conducted in a final volume of 20 μl with 1.5 U of ExTaq DNA polymerase (Takara Biomedicals)

and 250 nM each primer. Cycling conditions comprised a single denaturing step at 94°C for 10 min followed by 35 cycles of 94°C for 30 s, 60°C for 30 s, and 72°C for 1.5 min, followed by a final extension step of 72°C for 10 min. For *β-actin*, a single denaturing step at 94°C for 3 min was followed by 25 cycles of 94°C for 45 s, 50°C for 45 s, and 72°C for 1 min, followed by a final extension step of 72°C for 3 min (33).

Real-time PCR

Real-time PCR for quantification of *α-fodrin*, *Foxn1*, and tissue-specific Ag genes was conducted with thymic stroma cDNA prepared as described above. The primers and the probes are as follows. *α2-spectrin* primers: 5′-GACAGCCAGTGATGAGTCATACAAG-3′ and 5′-CACGGATTCGGTCAGCATT-3′; *α2-spectrin* probe: 5′-FAM-ACCCCACCAACATCCAGAGCAAGC-3′; *Foxn1* primers: 5′-GACATGCACCTCAGCACTCTCTA-3′ and 5′-CTGATGTTGGGCATAGCTCAAG-3′; *Foxn1* probe: 5′-FAM- CCCGGCTCAAAGCCATTGGCTC-3′; *insulin* primers: 5′-AGACCATCAGCAAGCAGGTC-3′ and 5′-CTGGTGCAGCACTGATCCAC-3′; *insulin* probe: 5′-FAM-CCCGGCAGAAGCGTGGCATT-3′; *salivary protein 1* primers: 5′-ACTCCTTGTGTTGCTTGGTGTTT-3′ and 5′-TCGACTGAATCAGAGGAATCAACT-3′; *salivary protein 1* probe: 5′-FAM-TTCACCAGCAGAATCAGCAGTTCCAGAA; *C-reactive protein* primers: 5′-TACTCTGGTGCCTTCTGATCATGA-3′ and 5′-GGCTTCTTTGACTCTGCTTCCA-3′; *C-reactive protein* probe: 5′-FAM-CAGCTTCTCTCGGACTTTTGGTCATGA-3′; *fatty acid binding protein* primers: 5′-CGTGTAGACAATGGAAAGGAGCT-3′ and 5′-AAGAATCGCTTGGCCTCAACT-3′; *fatty acid binding protein* probe: 5′-FAM-TCATTACCAGAAACCTCTCGGACAGCA-3′; *glutamic acid decarboxylase 67* primers: 5′-TCCTCCAAGAACCTGCTTTCC-3′ and 5′-GCTCCTCCCCGTTCTTAGCT-3′; *glutamic acid decarboxylase 67* probe: 5′-FAM-CCGACTTCTCCAACCTGTTTGCTCAAGA-3′. *Foxp3* expression was examined with cDNAs prepared from splenocytes ($CD4^+CD25^+$ or $CD4^+CD25^-$) and total thymus. The primers, the probes, and the reactions used for *Foxp3* and *Hprt* were those described previously (33, 34).

Thymus grafting

Thymus grafting was performed as previously performed (33). Briefly, thymic lobes were isolated from embryos at 14.5 days postcoitus, and then cultured for 4 days on Nucleopore filters (Whatman) placed on R10 containing 1.35 mM 2′-deoxyguanosine (Sigma-Aldrich). Five pieces of thymic lobes were grafted under the renal capsule of BALB/c *nude* mice. After 6–8 wk, reconstitution of peripheral T cells was determined by flow cytometric analysis with anti-CD4 (clone GK1.5; BD Pharmingen) and anti-CD8 (clone 53-6.7; BD Pharmingen) mAbs, and then the thymic chimeras were used for analysis.

Immunohistochemistry

Immunohistochemical analysis of the thymus was performed as described previously (35, 36). For the detection of auto-Abs, mouse serum was incubated with various organs obtained from Rag2-deficient mice. FITC-conjugated anti-mouse IgG Ab (Southern Biotechnology Associates) was used for the detection (33).

Isolation and functional analysis of Tregs

Spleen cell suspensions were stained with FITC-conjugated anti-CD25 (clone 7D4) and PE-conjugated anti-CD4 (clone H129.19) (BD Pharmingen), and sorted by FACS (ALTRA; Beckman Coulter) as described previously (37). The purity of the $CD25^-$ and $CD25^+CD4^+$ populations was >90 and 95%, respectively. Spleen cells sorted as described above were cocultured with RBC-lysed and irradiated (15 Gy) spleen cells (5×10^4) from wild-type mice as APC for 3 days in 96-well round-bottom plates in R10. Anti-CD3 mAb (clone 145-2C11) (Cedarlane Laboratories) at a final concentration of 10 μg/ml was added to the culture for stimulation, and ^3H incorporation during the last 6 h of culture was measured.

Results

Development of Sjögren's syndrome (SS)-like pathologic changes in exocrine organs from Aire-deficient mice

To investigate the roles of AIRE in the establishment and maintenance of self-tolerance in vivo, we generated Aire-null mutant mice. To this end, we deleted a large proportion of the known functional domains of *Aire* including SAND, PHD1, and PHD2 (6) (Fig. 1*A*). The correct targeted event was confirmed by Southern blot analysis and genomic PCR of material from the gene-targeted

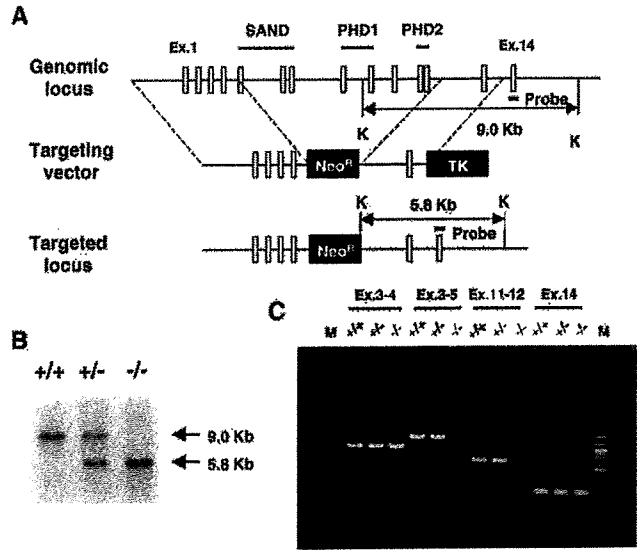

FIGURE 1. Generation of Aire-deficient mice. *A*, Targeted disruption of the gene encoding *Aire* by homologous recombination. K, *Kpn*I restriction site. *B*, Southern blot analysis of genomic DNA from offspring of heterozygous Aire-deficient mouse intercrosses. Tail DNA was digested with *Kpn*I and hybridized with a probe shown in *A*. *C*, Detection of genomic fragments of the *Aire* locus by PCR. Sequences spanning exons 5 and 12 were not amplified in tail DNA of homozygous Aire-deficient mice.

mice (Fig. 1, *B* and *C*). Offspring homozygous for Aire deficiency were born in the numbers expected from the heterozygous crossing, and homozygous Aire-deficient mice were grossly normal. Although both male and female homozygous Aire-deficient mice are fertile when crossed with wild-type mice, homozygous crossing produced offspring only occasionally (F. Kajiura and M. Matsumoto, unpublished observation). Total spleen cell numbers and total thymocyte numbers were indistinguishable between control and Aire-deficient mice. Flow cytometric analysis showed similar expression of B220, CD3, CD4, and CD8 in the spleen and thymus of control and Aire-deficient mice. Proliferative responses and Ig production from the B cells after various stimuli, and proliferative responses and IL-2 production from the T cells stimulated with anti-CD3 mAb, were also unchanged by the Aire deficiency (S. Sun and M. Matsumoto, unpublished observation).

To assess the impact of Aire deficiency on the breakdown of self-tolerance, we inspected various organs (i.e., salivary glands, lacrimal glands, thyroid, heart, lung, liver, stomach, pancreas, kidney, small intestine, testis, and ovary) from Aire-deficient mice of original mixed background (i.e., $H\text{-}2^{b/k} \times H\text{-}2^b$). The most marked changes were evident in the lacrimal glands (Fig. 2, *A* and *B*); all the Aire-deficient mice showed infiltration of many lymphoid cells in the lacrimal glands, whereas no such changes were observed in the control mice. We also observed infiltration of many lymphoid cells in the parotid glands (8 of 8 Aire-deficient mice) and submandibular glands (10 of 16 Aire-deficient mice) (Fig. 2*A*). Consistent with these SS-like pathologic changes in exocrine organs from Aire-deficient mice, secretion of tears per unit of mouse body weight was decreased in the affected mice (0.89 ± 0.33 mm/20 min/body weight (g) from control mice ($n = 5$) vs 0.46 ± 0.08 mm/20 min/body weight (g) from Aire-deficient mice ($n = 4$); $p < 0.05$). In 1 of 10 Aire-deficient mice, lymphoid cell infiltration in either the stomach or pancreas was also observed. There were no obvious pathologic changes in other organs from Aire-deficient mice during follow-up to the age of 8 mo.

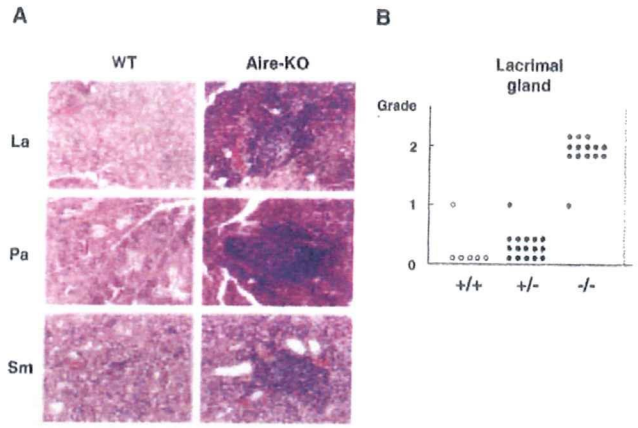

FIGURE 2. Development of organ-specific pathologic changes in Aire-deficient mice. *A*, Aire-deficient mice exhibited many infiltrating lymphoid cells in the lacrimal gland (La), parotid gland (Pa), and submandibular gland (Sm). In contrast, these changes were scarcely observed in control mice. Original magnification, ×100. *B*, Histological changes in H&E-stained tissue sections were scored as 0 (no change), 1 (mild lymphoid cell infiltration), or 2 (marked lymphoid cell infiltration). One mark corresponds to one mouse analyzed.

Autoreactive responses against α-fodrin in Aire-deficient mice

We have previously reported that NFS/*sld* mutant mice thymectomized 3 days after birth (3d-Tx) exhibit SS-like phenotypes with autoreactivity against α-fodrin, a ubiquitously expressed actin-binding protein (27, 38). Because of the similarity of SS-like phenotypes between Aire-deficient mice and the 3d-Tx-SS model, we investigated whether Aire-deficient mice exhibit autoreactivity against α-fodrin. We first tested the production of auto-Ab against various forms of recombinant α-fodrin in sera from Aire-deficient mice using Western blot analysis (Fig. 3, *A* and *B*). Sera from 3d-Tx mice showed reactivity predominantly against the JS-1 fragment (27). Four of five Aire-deficient mice showed reactivity against 2.7A, and two mice showed reactivity against 3′DA (Fig. 3*B*). Sera from control mice showed no such reactivities. Production of auto-Ab against α-fodrin in Aire-deficient mice was also evaluated by ELISA using additional forms of recombinant α-fodrin (31) and larger numbers of mice. Ten of 11 Aire-deficient mice showed significantly higher reactivities against at least one form of recombinant α-fodrin fragment compared with those from 11 control mice (Fig. 3*C*). Interestingly, each Aire-deficient mouse showed reactivity against different forms of α-fodrin.

We also confirmed the development of autoimmunity against α-fodrin using splenocytes from Aire-deficient mice (25). Such splenocytes cultured with recombinant α-fodrin showed significant proliferative responses; four Aire-deficient mice tested showed a response to 2.7A, but not to JS-1, whereas no such reactivities were observed from age-matched control mice (Fig. 4).

Unrepressed expression of corresponding target Ag in Aire-deficient thymus

The mechanism controlling the thymic microenvironment necessary for the establishment of self-tolerance in an Aire-dependent manner is of considerable interest. It has been suggested that "promiscuous" expression of a broad range of peripheral tissue-specific genes by TECs is essential for establishing self-tolerance (18), and Aire has been implicated in the control of this promiscuous gene expression through a transcriptional mechanism (19). Supporting this notion, real-time PCR has revealed that expression of *insulin*

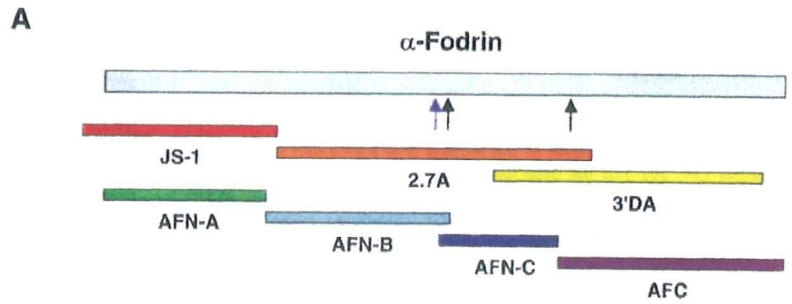

C

KO	JS-1	2.7A	3′DA	AFN-A	AFN-B	AFN-C	AFC
1	0.052	0.196	0.081	0.053	0.435	0.088	0.074
2	0.620	0.171	0.034	0.043	0.227	0.076	0.066
3	0.084	0.094	0.050	0.099	0.089	0.051	0.157
4	0.186	0.058	0.058	0.093	0.187	0.047	0.213
5	0.043	0.057	0.037	0.059	0.103	[illegible]	0.110
6	0.028	0.027	0.057	0.023	0.055	0.045	0.081
7	0.339	0.095	0.035	0.050	0.082	[illegible]	0.072
8	0.178	0.034	0.034	0.071	0.062	0.044	0.076
9	0.084	0.178	0.037	0.079	0.259	0.054	0.307
10	0.053	0.083	0.865	0.020	0.136	0.038	0.796
11	0.264	0.060	0.046	0.151	0.103	[illegible]	0.075

FIGURE 3. Production of auto-Abs against α-fodrin in Aire-deficient mice. *A*, Schematic representation of α-fodrin. Black arrows and a blue arrow show the sites of cleavage by caspase 3 and calpain, respectively. *B*, Western blot analysis for recombinant α-fodrin with Aire-deficient mouse sera. Representative results from two mice from both wild-type and Aire-deficient mice are shown. Serum from NFS/*sld* mutant 3d-Tx mice reacted predominantly with the JS-1 fragment. 1, JS-1; 2, 2.7A; 3, 3′DA. *C*, Detection of auto-Abs against various forms of α-fodrin in sera from Aire-deficient mice using ELISA. Absorbance values greater than the mean ± 3 SD in wild-type mouse sera were considered positive and are colored.

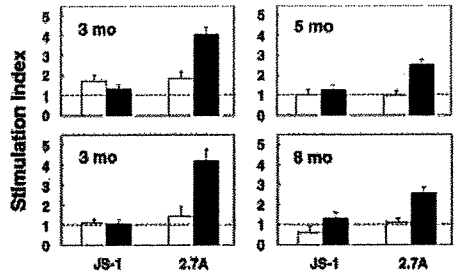

FIGURE 4. Autoreactive responses against α-fodrin by splenocytes from Aire-deficient mice. Proliferative responses of total splenocytes against two forms of recombinant α-fodrin (shown in Fig. 3*A*) were determined, and stimulation indices are demonstrated from control mice (open bars) and Aire-deficient mice (filled bars). Ages of the mice used are indicated.

and *salivary protein 1* was significantly reduced in the Aire-deficient thymic stroma (Fig. 5*A*). Because Aire-deficient mice developed autoimmunity against the defined target Ag, α-fodrin, we examined whether the expression of α-fodrin mRNA in the thymic stroma is changed in Aire-deficient mice. Using real-time PCR together with semiquantitative RT-PCR with three sets of primers encompassing the entire coding region of *α-fodrin*, we detected unrepressed *α-fodrin* expression from Aire-deficient thymic stroma when compared with that from control thymic stroma (Fig. 5, *A* and *B*); this was observed under the condition where the expression of *Foxn1*, which encodes a transcription factor involved in thymus development (39), was indistinguishable between the samples (Fig. 5*A*). Thus, our results suggest that Aire regulates self-tolerance beyond the transcriptional control of self-protein expression in the thymus, at least against this ubiquitously expressed protein.

To test whether autoreactivity against α-fodrin is associated with the development of inflammatory lesions in exocrine organs from Aire-deficient mice, we performed Western blot analysis using proteins extracted from the lacrimal glands. Both lacrimal glands and thymus from younger Aire-deficient mice (i.e., 3 mo) contained larger quantities of intact form α-fodrin (240 kDa) than the cleaved form (150 kDa), as observed for proteins from the control mice (Fig. 6*A*); this was demonstrated with two different kinds of Abs recognizing the C-terminal half (anti-α-fodrin mAb) and N-terminal half (anti-AFN-A polyclonal Ab) of α-fodrin. However, lacrimal glands from some aged Aire-deficient mice (i.e., 8 mo) contained a reduced amount of the intact form (Fig. 6*B*), although no detectable changes in α-fodrin expression in the thymus were observed in either form or quantity. This result suggests that autoreactivity against α-fodrin is associated with the pathogenetic process responsible for destruction of the lacrimal glands in this SS-like model, as observed in 3d-Tx-SS model (27, 38).

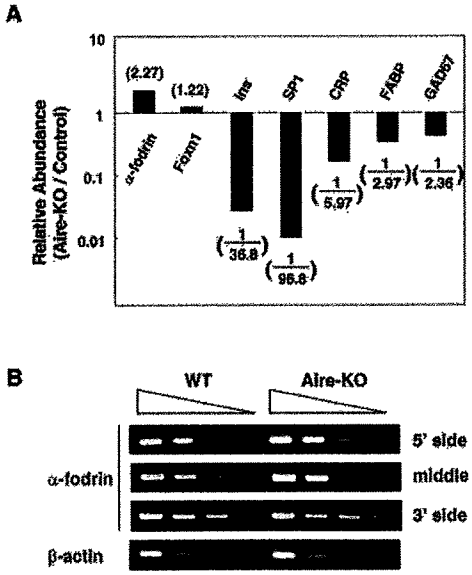

FIGURE 5. Unrepressed target Ag expression from Aire-deficient thymus. *A*, Real-time PCR for *α-fodrin*, *Foxn1*, and peripheral tissue-specific genes (i.e., Ins, *insulin*; SP1, *salivary protein 1*; CRP, *C-reactive protein*; FABP, *fatty acid-binding protein*; GAD67, *glutamic acid decarboxylase 67*) was performed using thymic-stroma RNAs from control and Aire-deficient mice. *Hprt* expression level was used as an internal control. Relative abundance of each gene was calculated from the ratio between the values from control thymus and those from Aire-deficient thymus (e.g., *insulin/Hprt* value from Aire-deficient mice was divided by *insulin/Hprt* value from control mice) and is shown in parentheses. One representative result from a total of three repeats is shown. *B*, Semiquantitative RT-PCR for *α-fodrin* was performed using thymic-stroma RNAs from control and Aire-deficient mice. *β-Actin* was used to verify equal amounts of RNAs in each sample. Three sets of primers encompassing the entire coding region of *α-fodrin* were used for detection. One representative result from a total of three repeats is shown.

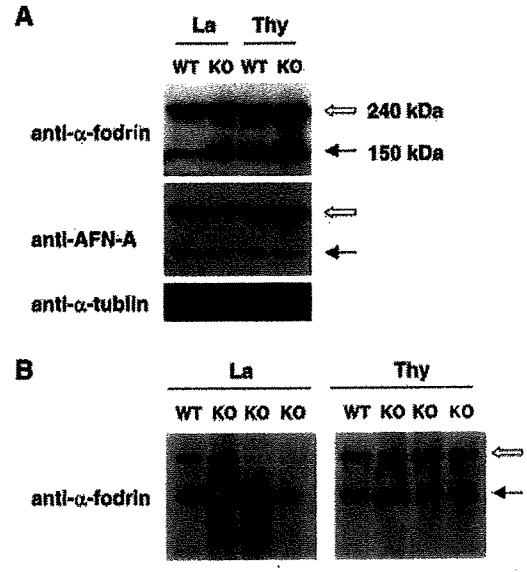

FIGURE 6. Autoreactivity against α-fodrin is associated with the pathogenetic process responsible for destruction of the lacrimal glands. *A*, Proteins extracted from the lacrimal glands and thymus of 3-mo-old mice were subjected to Western blot analysis using two different kinds of Abs recognizing the C-terminal half (anti-α-fodrin Ab, *top*) and N-terminal half (anti-AFN-A Ab, *center*) of α-fodrin. Open and filled arrows indicate the 240-kDa intact form and 150-kDa cleaved form of α-fodrin, respectively. The same blot was probed with anti-α-tubulin Ab (*bottom*). La, lacrimal gland; Thy, thymus. *B*, Proteins were extracted from the lacrimal glands and thymus of 8-mo-old mice. Western blot analysis was performed as shown in *A*. Lacrimal glands from some of the Aire-deficient mice showed a markedly reduced amount of the intact form (*left panel*, third and fourth lanes), although Aire-deficient thymus showed no detectable changes in α-fodrin expression in terms of form or quantity compared with control thymus (*right panel*). Open and filled arrows indicate the 240-kDa intact form and 150-kDa cleaved form of α-fodrin, respectively.

Loss of Aire in the thymic stroma is responsible for the breakdown of self-tolerance

Despite the predominant Aire expression in TECs, thymic structure was not apparently affected by the absence of Aire. Results of H&E staining as well as immunohistochemistry with the lectin *Ulex europaeus* agglutinin 1 (40) and ER-TR5 mAb (41), both recognizing a subset of mTEC, were indistinguishable between control and Aire-deficient mice (F. Kajiura, T. Ueno, Y. Takahama, and M. Matsumoto, unpublished observation). Organization of dendritic cells in the thymus identified with the mAb CD11c was also unaffected by Aire deficiency. Thus, Aire may not affect thymic organogenesis. Alternatively, relatively low frequencies of Aire-expressing cells among mTECs may account for the apparently normal thymic structure in Aire-deficient mice.

To investigate the impact of Aire deficiency in the thymic microenvironment, we generated thymic chimeras. Thymic lobes were isolated from control and Aire-deficient embryos of mixed background ($H\text{-}2^{b/k} \times H\text{-}2^{b}$) and cultured for 4 days in the presence of 2′-deoxyguanosine to eliminate thymocytes. Such thymic lobes did not contain any live thymocytes, as determined by flow cytometric analysis and Western blot analysis with anti-lck Ab (33). The lobes were then grafted under the renal capsule of BALB/c *nude* mice ($H\text{-}2^{d}$). Grafting of both control and Aire-deficient embryonic thymus induced T cell maturation in BALB/c *nude* mice at the periphery to a similar extent: $CD4^+$ T cells plus $CD8^+$ T cells were 12.5 ± 2.2% in *nude* mice grafted with control thymus ($n = 6$), compared with 12.3 ± 1.6% in *nude* mice grafted with Aire-deficient thymus ($n = 7$). It is important to note that the mature T cells produced de novo in both cases originated from Aire-sufficient *nude* mouse bone marrow (BM). Remarkably, histological examination of Aire-deficient thymus-grafted mice revealed infiltration of many lymphoid cells in the liver (mainly in the portal area) and pancreas (interlobular periductal and perivascular areas near islets) (Fig. 7, *A* and *B*). In contrast, we observed few such changes in control thymus-grafted mice.

To confirm that T cells developing in a thymic microenvironment without Aire are autoreactive per se, we injected splenocytes obtained from BALB/c *nude* mice grafted with Aire-deficient thymus into another group of BALB/c *nude* mice. We observed similar lymphoid cell infiltration in the liver of the recipient mice, whereas injection of splenocytes obtained from *nude* mice grafted with control thymus induced no such changes in the recipient mice (Fig. 7*B*). These results clearly indicate the significance of Aire as a thymic stromal element required for the establishment of self-tolerance.

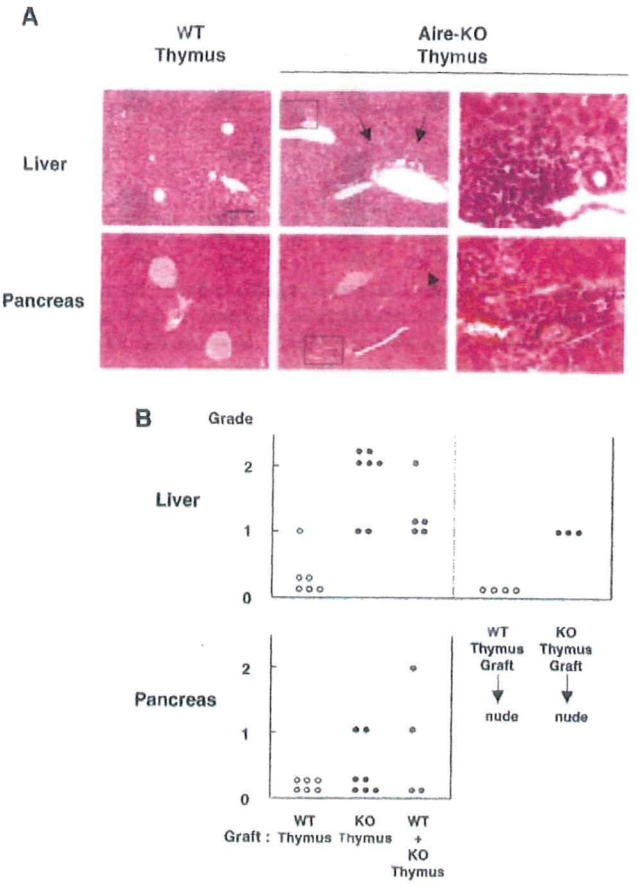

FIGURE 7. Thymic stromal elements in Aire-deficient mice are responsible for the development of autoimmunity. *A*, BALB/c *nude* mice grafted with Aire-deficient embryonic thymus (*middle panels*), but not with control embryonic thymus (*left panels*), developed an autoimmune disease phenotype in the liver and pancreas. The indicated areas are magnified in the *right panels*. Arrows indicate lymphoid cell infiltration. The scale bar corresponds to 100 μm. *B*, Many Aire-deficient thymus-grafted BALB/c *nude* mice exhibited lymphoid cell infiltration in the liver (*top*) and pancreas (*bottom*). In contrast, such changes were scarcely observed in mice grafted with control thymus. BALB/c *nude* mice grafted with both Aire-deficient thymus and control thymus showed significant pathological changes. Injection of splenocytes from BALB/c *nude* mice grafted with Aire-deficient thymus, but not with control thymus, into another group of BALB/c *nude* mice induced lymphoid cell infiltration in the liver of the recipient mice. Histological changes in H&E-stained tissue sections were scored as shown in Fig. 2*B*. One mark corresponds to one mouse analyzed.

Impaired regulation of autoreactivity in the absence of Aire

There is accumulating evidence that T cell-mediated dominant control of autoreactive T cells represents an important mechanism for the maintenance of immunologic self-tolerance (16, 17). We investigated whether loss of Aire in the thymus has a major impact on the production and/or function of Tregs. Spleen and thymus from adult Aire-deficient mice contained similar percentages as well as total numbers of $CD4^+CD25^+$ T cells compared with those from control mice (Fig. 8*A*). Real-time PCR for quantification of *Foxp3* mRNA (34, 42, 43) did not show any reduction of Tregs in the spleen of Aire-deficient mice (Fig. 8*B*). Expression of *Foxp3* in the whole thymus was also comparable between control mice and Aire-deficient mice (*Foxp3/Hprt* from wild-type mice = 1.8 vs *Foxp3/Hprt* from Aire-deficient mice = 2.4).

Recently, it has been demonstrated that functional alterations of Tregs could contribute to the development of autoimmune disease. A significant decrease in the effector function of $CD4^+CD25^+$ T cells from peripheral blood of patients with multiple sclerosis has been reported (44). It is of particular interest that the suppressor function of $CD4^+CD25^+$ T cells has been demonstrated to be defective in patients with autoimmune polyglandular syndrome type II, which is phenotypically closely related to APECED (also called autoimmune polyglandular syndrome type I) but whose pathogenesis is currently unknown (45). It is therefore important to test the function of Tregs from Aire-deficient mice. $CD4^+CD25^+$ T cells isolated from Aire-deficient mice dose-dependently suppressed [^{3}H]thymidine uptake by naive T cells cocultured in vitro with an efficiency nearly identical to that of $CD4^+CD25^+$ cells from control mice (Fig. 8*Ca*). This was also the case when responder cells ($CD4^+CD25^-$ cells) isolated from Aire-deficient mice were used for the assay (Fig. 8*Cb*). Thus, Aire does not have a major impact on the production and/or function of Tregs, at least as assessed in those assays.

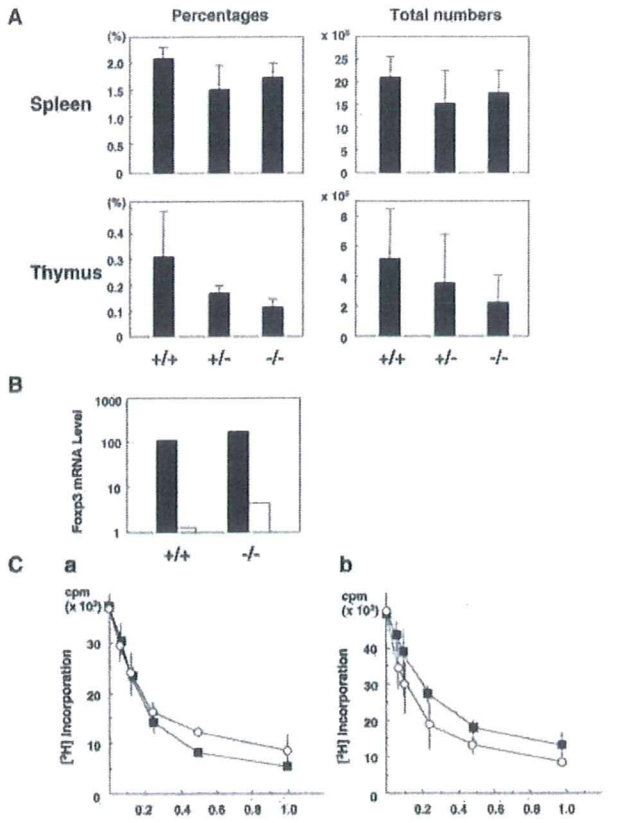

FIGURE 8. Retained production and function of Tregs from Aire-deficient mice. *A*, Spleens and thymuses from Aire-deficient mice contained percentages as well as total numbers of $CD4^+CD25^+$ T cells indistinguishable from those of control mice. $n = 5$, not statistically significant. *B*, Real-time PCR for *Foxp3* expression was performed using RNAs extracted from purified $CD4^+CD25^+$ (filled bars) and $CD4^+CD25^-$ T cells (open bars) with *Hprt* expression level as an internal control for the assay. One representative result from a total of two repeats is shown. *C*, $CD4^+CD25^+$ T cells isolated from Aire-deficient mice (*a*, ■) dose-dependently suppressed [^{3}H]thymidine uptake by native T cells from wild-type mice cocultured in vitro with an efficiency nearly identical to that of $CD4^+CD25^+$ cells from control mice (○). $CD4^+CD25^-$ T cells (2.5×10^4) were mixed with $CD4^+CD25^+$ T cells in various ratios as indicated on the *x*-axis. $CD4^+CD25^-$ T cells (2.5×10^4) were isolated from Aire-deficient mice (*b*), and their suppressive function was examined as shown in *a*. One representative result from a total of two repeats is shown.

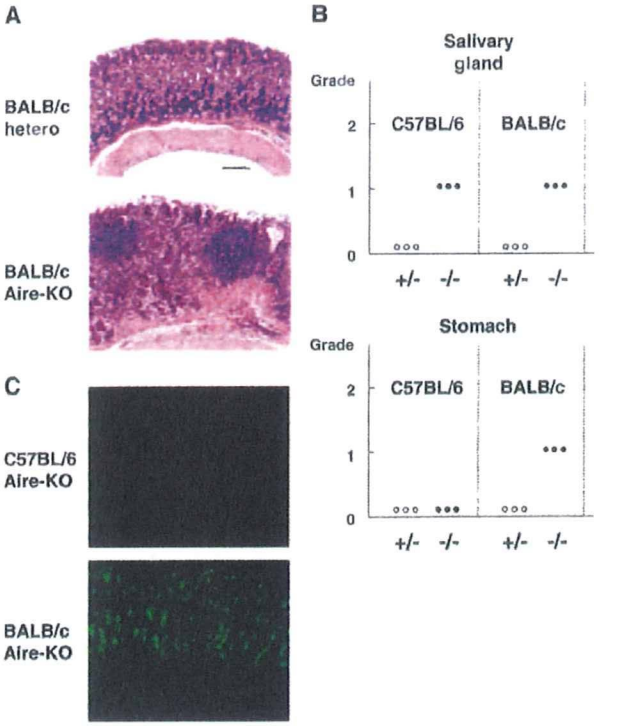

FIGURE 9. Strain-dependent target-organ specificity of the autoimmune disease caused by Aire deficiency. *A*, Aire-deficient BALB/c mice demonstrated lymphoid cell infiltration in the gastric mucosa (*bottom*). A scale bar corresponds to 100 μm in size (*top*; heterozygous Aire-deficient BALB/c mice). *B*, Aire-deficient BALB/c mice, but not Aire-deficient C57BL/6 mice, developed gastritis (*bottom*), whereas pathologic changes in the salivary glands were similarly observed in both strains (*top*). Histological changes in H&E-stained tissue sections were scored as shown in Fig. 2*B*. *C*, Aire-deficient BALB/c mice, but not Aire-deficient C57BL/6 mice, produced auto-Abs against gastric mucosa. Original magnification, ×100.

To gain further insight into how Aire contributes to the establishment of self-tolerance, we grafted control (Aire sufficient) and Aire-deficient embryonic thymus simultaneously into BALB/c *nude* mice. Inflammatory changes in the liver and pancreas of these animals were still present (Fig. 7*B*), supporting the hypothesis that impaired dominant control of autoreactive T cells by Tregs may not be the major defect caused by a thymic stroma lacking Aire; if impaired production of Tregs were the major defect caused by a thymic stroma lacking Aire, we assume that the defect should have been corrected by the grafted Aire-sufficient thymus. Therefore, it is reasonable to speculate that overproduction of autoreactive T cells plays an important role in the disease process triggered by Aire deficiency.

Strain-dependent target-organ specificity of the autoimmune disease caused by Aire deficiency

Although APECED is a monogenic disorder, it has been postulated that there may be additional factor(s) that determine the clinical features of the disease, such as the spectrum of affected organs (5, 6, 22). To test this hypothesis, we backcrossed our original strain of Aire-deficient mice to either the C57BL/6 (H-2^b) or BALB/c (H-2^d) strain for six generations. Both backcrossed strains showed autoimmune phenotypes similar to those from an original strain of Aire-deficient mice of mixed background (i.e., infiltration of many lymphoid cells in the salivary glands) (Fig. 9*B*, *top*). However, Aire-deficient BALB/c mice additionally demonstrated lymphoid cell infiltration in the gastric mucosa (Fig. 9, *A* and *B*, *bottom*), a feature that has been observed only rarely in the original Aire-deficient mice of mixed background (1 of 10) or Aire-deficient C57BL/6 mice (Fig. 9*B*, *bottom*). Consistent with these histological findings, serum harvested from Aire-deficient BALB/c mice (4 of 4) demonstrated strong auto-Abs against gastric mucosa (Fig. 9*C*), whereas this activity was observed in only one of four Aire-deficient C57BL/6 mice, and it was weak. Thus, the genetic background of the mice clearly influences the target-organ specificity of the disease caused by Aire deficiency.

Discussion

Using gene-targeted mice, we have investigated the mechanisms controlling the establishment and maintenance of self-tolerance by Aire. Both the numbers and suppressive function of $CD4^+CD25^+$ Tregs were not changed in Aire-deficient mice, when assessed in the adult mice. Using thymic chimeras, we also investigated possible defects in the production of any cell types (including

$CD4^+CD25^+$ Tregs) that are involved in the prevention of T cell-mediated organ-specific autoimmune diseases in the absence of Aire. When Aire-deficient and Aire-sufficient thymus were grafted simultaneously into *nude* mice, the development of inflammatory lesions was not completely inhibited. These results suggest that impaired production of Tregs may not be the major mechanism responsible for the breakdown of self-tolerance in Aire-deficient mice, and it is reasonable to speculate that the Aire-deficient thymus allows production of more pathogenic autoreactive T cells than could be controlled by the Tregs. However, it is important to emphasize that other aspects of Tregs, such as their repertoire formation, still remain unsolved; we cannot rule out the possibility that Aire may affect the Ag specificity of the Treg repertoire, because most of the analysis of the Tregs in the present study was quantitative rather than qualitative.

We have demonstrated that anti-α-fodrin autoimmunity developed in Aire-deficient mice despite the fact that the transcription of corresponding Ag (i.e., α-fodrin) in the thymic stroma was not down-regulated. Based on this finding, we suggest that Aire may regulate the processing and/or presentation of self-Ags by TECs, possibly through a coordinated action with BM-derived cells (see below), so that the maturing T cells can recognize the corresponding self-Ags in a form capable of efficiently triggering autoreactive T cells. It would be important to know whether our proposed model of Aire function in the establishment of self-tolerance is confined to ubiquitous self-Ags, such as α-fodrin, or applicable to tissue-specific Ags as well. In this regard, it is critical to investigate first whether autoimmunity develops bona fide against transcriptionally repressed tissue-specific Ags in the thymus in Aire-deficient mice. Definitively, identification of the substrate(s) for E3 ubiquitin ligase activity by AIRE should help to clarify the actual mechanisms of AIRE-dependent tolerance (10).

We have demonstrated that α-fodrin is one of the target Ags involved in the autoimmune-disease process caused by Aire deficiency. Because transfer of sera from affected mice did not result in the development of sialoadenitis or disruption of α-fodrin in the recipient mice (N. Ishimaru, R. Arakaki, and Y. Hayashi, unpublished observation), the disease process in Aire-deficient mice is most likely elicited by a cell-mediated immunity, as observed in the 3d-Tx-SS model (29, 30). Consistent with this hypothesis, splenocytes from Aire-deficient mice demonstrated proliferative responses in vitro when cultured with recombinant α-fodrin (Fig. 4).

Reduction of the intact form of α-fodrin in the affected lacrimal glands of some aged Aire-deficient mice (Fig. 6*B*) suggests that elicitation of autoreactivity against α-fodrin could be the primary pathogenetic process that leads to tissue destruction (27). In fact, adoptive transfer of α-fodrin-reactive T cells into ovariectomized B6 and SCID mice resulted in the development of autoimmune exocrinopathy quite similar to SS (30). However, based on the fact that α-fodrin is a ubiquitous protein and that the tissue destruction is confined to exocrine organs, it is reasonable to speculate that other undetermined tissue-specific target Ag(s) in exocrine organs might be additionally involved in the tissue destruction. Identification of precise target Ags involved in the disease process in Aire-deficient mice should help unravel the molecular mechanisms by which loss of Aire contributes to disease development.

We have demonstrated Aire-dependent disease development using allogeneic thymic chimeras; autoimmune disease commences in BALB/c *nude* recipients ($H\text{-}2^d$) of Aire-deficient, but not of wild-type, thymic transplants from mice of original mixed background ($H\text{-}2^{b/k} \times H\text{-}2^b$) (Fig. 7). The roles of TECs vs BM-derived cells in T cell repertoire selection in allogeneic thymic chimeras have been an issue of long-standing interest and debate. Given that *nude* mice reconstituted with an MHC-incompatible thymus generate effector T cells that are specific for the host and not for the thymic MHC (46), a novel mechanism may be responsible for the Aire-dependent negative selection; Aire expressed on TECs acts on BM-derived cells "in trans" as an important factor in organizing the "negative selection niche" in the thymus (47). This scenario is in good accordance with our results demonstrating the impaired tolerance to a ubiquitously expressed auto-Ag (i.e., α-fodrin) in Aire-deficient mice, because tolerance to ubiquitous self-proteins is mediated mainly by BM-derived cells in the thymus (48). Further study is required to test this intriguing hypothesis.

There is increasing evidence for the genetic complexity that underlies monogenic diseases (49, 50). In fact, the spectrum of the APECED phenotype is broad; the number of symptoms as well as the onset of each manifestation varies among affected patients. In our backcrossed mice, gastritis was observed predominantly in the BALB/c strain. In light of the fact that the individual HLA class II alleles modify the APECED phenotype (22), it is possible to speculate that MHC could be a candidate for the factor that determines this target-organ specificity. However, a genetic study with congenic strains has demonstrated that BALB/c ($H\text{-}2^d$), BALB.B ($H\text{-}2^b$), and BALB.K ($H\text{-}2^k$) were all susceptible to experimentally induced gastritis, whereas B10.D2 ($H\text{-}2^d$) were resistant, suggesting the predominant role of non-MHC gene(s) in determining susceptibility to autoimmune gastritis (51). Thus, MHC genes as well as non-MHC genes may together contribute to the complex phenotypes of APECED.

In conclusion, integration of detailed phenotypic analyses of Aire-deficient mice with current perspectives of thymus biology promises to illuminate many aspects of the molecular mechanisms responsible for the establishment and maintenance of self-tolerance. With the production of inbred strains of Aire-deficient mice, it may also be feasible to assess the impact of environmental factors that could influence the clinical features of APECED.

Acknowledgments

We thank Drs. W. van Ewijk and M. Itoi for the gift of ER-TR5 mAb. We thank Drs. T. Yamada, T. Yabuki, M. Kasai, and K. Iwabuchi for valuable suggestions. We also thank K. Awahayashi and F. Saito for technical assistance.

References

1. Kamradt, T., and N. A. Mitchison. 2001. Tolerance and autoimmunity. *N. Engl. J. Med. 344:655.*
2. Wanstrat, A., and E. Wakeland. 2001. The genetics of complex autoimmune diseases: non-MHC susceptibility genes. *Nat. Immunol. 2:802.*
3. Nagamine, K., P. Peterson, H. S. Scott, J. Kudoh, S. Minoshima, M. Heino, K. J. Krohn, M. D. Lalioti, P. E. Mullis, S. E. Antonarakis, et al. 1997. Positional cloning of the APECED gene. *Nat. Genet. 17:393.*
4. The Finnish-German APECED Consortium. 1997. An autoimmune disease, APECED, caused by mutations in a novel gene featuring two PHD-type zinc-finger domains. *Nat. Genet. 17:399.*
5. Björses, P., J. Aaltonen, N. Horelli-Kuitunen, M. L. Yaspo, and L. Peltonen. 1998. Gene defect behind APECED: a new clue to autoimmunity. *Hum. Mol. Genet. 7:1547.*
6. Pitkänen, J., and P. Peterson. 2003. Autoimmune regulator: from loss of function to autoimmunity. *Genes Immun. 4:12.*
7. Pitkänen, J., V. Doucas, T. Sternsdorf, T. Nakajima, S. Aratani, K. Jensen, H. Will, P. Vahamurto, J. Ollila, M. Vihinen, et al. 2000. The autoimmune regulator protein has transcriptional transactivating properties and interacts with the common coactivator CREB-binding protein. *J. Biol. Chem. 275:16802.*
8. Kumar, P. G., M. Laloraya, C. Y. Wang, Q. G. Ruan, A. Davoodi-Semiromi, K. J. Kao, and J. X. She. 2001. The autoimmune regulator (AIRE) is a DNA-binding protein. *J. Biol. Chem. 276:41357.*
9. Coscoy, L., and D. Ganem. 2003. PHD domains and E3 ubiquitin ligases: viruses make the connection. *Trends Cell Biol. 13:7.*
10. Uchida, D., S. Hatakeyama, A. Matsushima, H. Han, S. Ishido, H. Hotta, J. Kudoh, N. Shimizu, V. Doucas, K. I. Nakayama, et al. 2004. AIRE functions as an E3 ubiquitin ligase. *J. Exp. Med. 199:167.*
11. Hochstrasser, M. 1996. Ubiquitin-dependent protein degradation. *Annu. Rev. Genet. 30:405.*
12. Pickart, C. M. 2001. Mechanisms underlying ubiquitination. *Annu. Rev. Biochem. 70:503.*

13. Björses, P., M. Pelto-Huikko, J. Kaukonen, J. Aaltonen, L. Peltonen, and I. Ulmanen. 1999. Localization of the APECED protein in distinct nuclear structures. *Hum. Mol. Genet. 8:259.*
14. Heino, M., P. Peterson, J. Kudoh, K. Nagamine, A. Lagerstedt, V. Ovod, A. Ranki, I. Rantala, M. Nieminen, J. Tuukkanen, et al. 1999. Autoimmune regulator is expressed in the cells regulating immune tolerance in thymus medulla. *Biochem. Biophys. Res. Commun. 257:821.*
15. Kisielow, P., H. Bluthmann, U. D. Staerz, M. Steinmetz, and H. von Boehmer. 1988. Tolerance in T-cell-receptor transgenic mice involves deletion of nonmature $CD4^+8^+$ thymocytes. *Nature 333:742.*
16. Sakaguchi, S. 2004. Naturally arising $CD4^+$ regulatory T cells for immunologic self-tolerance and negative control of immune responses. *Annu. Rev. Immunol. 22:531.*
17. Shevach, E. M. 2002. $CD4^+CD25^+$ suppressor T cells: more questions than answers. *Nat. Rev. Immunol. 2:389.*
18. Kyewski, B., J. Derbinski, J. Gotter, and L. Klein. 2002. Promiscuous gene expression and central T-cell tolerance: more than meets the eye. *Trends Immunol. 23:364.*
19. Anderson, M. S., E. S. Venanzi, L. Klein, Z. Chen, S. Berzins, S. J. Turley, H. von Boehmer, R. Bronson, A. Dierich, C. Benoist, and D. Mathis. 2002. Projection of an immunological self-shadow within the thymus by the Aire protein. *Science 298:1395.*
20. Liston, A., S. Lesage, J. Wilson, L. Peltonen, and C. C. Goodnow. 2003. Aire regulates negative selection of organ-specific T cells. *Nat. Immunol. 4:350.*
21. Ramsey, C., O. Winqvist, L. Puhakka, M. Halonen, A. Moro, O. Kampe, P. Eskelin, M. Pelto-Huikko, and L. Peltonen. 2002. Aire deficient mice develop multiple features of APECED phenotype and show altered immune response. *Hum. Mol. Genet. 11:397.*
22. Halonen, M., P. Eskelin, A. G. Myhre, J. Perheentupa, E. S. Husebye, O. Kampe, F. Rorsman, L. Peltonen, I. Ulmanen, and J. Partanen. 2002. AIRE mutations and human leukocyte antigen genotypes as determinants of the autoimmune polyendocrinopathy-candidiasis-ectodermal dystrophy phenotype. *J. Clin. Endocrinol. Metab. 87:2568.*
23. Yagi, T., T. Tokunaga, Y. Furuta, S. Nada, M. Yoshida, T. Tsukada, Y. Saga, N. Takeda, Y. Ikawa, and S. Aizawa. 1993. A novel ES cell line, TT2, with high germline-differentiating potency. *Anal. Biochem. 214:70.*
24. Delporte, C., B. C. O'Connell, X. He, H. E. Lancaster, A. C. O'Connell, P. Agre, and B. J. Baum. 1997. Increased fluid secretion after adenoviral-mediated transfer of the aquaporin-1 cDNA to irradiated rat salivary glands. *Proc. Natl. Acad. Sci. USA 94:3268.*
25. Saegusa, K., N. Ishimaru, K. Yanagi, R. Arakaki, K. Ogawa, I. Saito, N. Katunuma, and Y. Hayashi. 2002. Cathepsin S inhibitor prevents autoantigen presentation and autoimmunity. *J. Clin. Invest. 110:361.*
26. Moon, R. T., and A. P. McMahon. 1990. Generation of diversity in nonerythroid spectrins. Multiple polypeptides are predicted by sequence analysis of cDNAs encompassing the coding region of human nonerythroid α-spectrin. *J. Biol. Chem. 265:4427.*
27. Haneji, N., T. Nakamura, K. Takio, K. Yanagi, H. Higashiyama, I. Saito, S. Noji, H. Sugino, and Y. Hayashi. 1997. Identification of α-fodrin as a candidate autoantigen in primary Sjögren's syndrome. *Science 276:604.*
28. Saegusa, K., N. Ishimaru, K. Yanagi, K. Mishima, R. Arakaki, T. Suda, I. Saito, and Y. Hayashi. 2002. Prevention and induction of autoimmune exocrinopathy is dependent on pathogenic autoantigen cleavage in murine Sjögren's syndrome. *J. Immunol. 169:1050.*
29. Arakaki, R., N. Ishimaru, I. Saito, M. Kobayashi, N. Yasui, T. Sumida, and Y. Hayashi. 2003. Development of autoimmune exocrinopathy resembling Sjögren's syndrome in adoptively transferred mice with autoreactive $CD4^+$ T cells. *Arthritis Rheum. 48:3603.*
30. Ishimaru, N., R. Arakaki, M. Watanabe, M. Kobayashi, K. Miyazaki, and Y. Hayashi. 2003. Development of autoimmune exocrinopathy resembling Sjögren's syndrome in estrogen-deficient mice of healthy background. *Am. J. Pathol. 163:1481.*
31. Ogawa, K., S. Nagahiro, R. Arakaki, N. Ishimaru, M. Kobayashi, and Y. Hayashi. 2003. Anti-α-fodrin autoantibodies in Moyamoya disease. *Stroke 34:e244.*
32. Gray, D. H., A. P. Chidgey, and R. L. Boyd. 2002. Analysis of thymic stromal cell populations using flow cytometry. *J. Immunol. Methods 260:15.*
33. Kajiura, F., S. Sun, T. Nomura, K. Izumi, T. Ueno, Y. Bando, N. Kuroda, H. Han, Y. Li, A. Matsushima, et al. 2004. NF-κB-inducing kinase establishes self-tolerance in a thymic stroma-dependent manner. *J. Immunol. 172:2067.*
34. Hori, S., T. Nomura, and S. Sakaguchi. 2003. Control of regulatory T cell development by the transcription factor FOXP3. *Science 299:1057.*
35. Matsumoto, M., Y.-X. Fu, H. Molina, G. Huang, J. Kim, D. A. Thomas, M. H. Nahm, and D. D. Chaplin. 1997. Distinct roles of lymphotoxin α and the type I tumor necrosis factor (TNF) receptor in the establishment of follicular dendritic cells from non-bone marrow-derived cells. *J. Exp. Med. 186:1997.*
36. Yamada, T., T. Mitani, K. Yorita, D. Uchida, A. Matsushima, K. Iwamasa, S. Fujita, and M. Matsumoto. 2000. Abnormal immune function of hemopoietic cells from alymphoplasia (*aly*) mice, a natural strain with mutant NF-κB-inducing kinase. *J. Immunol. 165:804.*
37. Itoh, M., T. Takahashi, N. Sakaguchi, Y. Kuniyasu, J. Shimizu, F. Otsuka, and S. Sakaguchi. 1999. Thymus and autoimmunity: production of $CD25^+CD4^+$ naturally anergic and suppressive T cells as a key function of the thymus in maintaining immunologic self-tolerance. *J. Immunol. 162:5317.*
38. Haneji, N., H. Hamano, K. Yanagi, and Y. Hayashi. 1994. A new animal model for primary Sjögren's syndrome in NFS/*sld* mutant mice. *J. Immunol. 153:2769.*
39. Nehls, M., B. Kyewski, M. Messerle, R. Waldschutz, K. Schuddekopf, A. J. Smith, and T. Boehm. 1996. Two genetically separable steps in the differentiation of thymic epithelium. *Science 272:886.*
40. Farr, A. G., and S. K. Anderson. 1985. Epithelial heterogeneity in the murine thymus: fucose-specific lectins bind medullary epithelial cells. *J. Immunol. 134:2971.*
41. Van Vliet, E., M. Melis, and W. van Ewijk. 1984. Monoclonal antibodies to stromal cell types of the mouse thymus. *Eur. J. Immunol. 14:524.*
42. Fontenot, J. D., M. A. Gavin, and A. Y. Rudensky. 2003. Foxp3 programs the development and function of $CD4^+CD25^+$ regulatory T cells. *Nat. Immunol. 4:330.*
43. Khattri, R., T. Cox, S. A. Yasayko, and F. Ramsdell. 2003. An essential role for Scurfin in $CD4^+CD25^+$ T regulatory cells. *Nat. Immunol. 4:337.*
44. Viglietta, V., C. Baecher-Allan, H. L. Weiner, and D. A. Hafler. 2004. Loss of functional suppression by $CD4^+CD25^+$ regulatory T cells in patients with multiple sclerosis. *J. Exp. Med. 199:971.*
45. Kriegel, M. A., T. Lohmann, C. Gabler, N. Blank, J. R. Kalden, and H. M. Lorenz. 2004. Defective suppressor function of human $CD4^+CD25^+$ regulatory T cells in autoimmune polyglandular syndrome type II. *J. Exp. Med. 199:1285.*
46. Zinkernagel, R. M., and A. Althage. 1999. On the role of thymic epithelium vs. bone marrow-derived cells in repertoire selection of T cells. *Proc. Natl. Acad. Sci. USA 96:8092.*
47. Kyewski, B., and J. Derbinski. 2004. Self-representation in the thymus: an extended view. *Nat. Rev. Immunol. 4:688.*
48. Sprent, J., and C. D. Surh. 2003. Knowing one's self: central tolerance revisited. *Nat. Immunol. 4:303.*
49. Estivill, X. 1996. Complexity in a monogenic disease. *Nat. Genet. 12:348.*
50. Weatherall, D. J. 2000. Single gene disorders or complex traits: lessons from the thalassaemias and other monogenic diseases. *Br. Med. J. 321:1117.*
51. Sakaguchi, S., and N. Sakaguchi. 2000. Role of genetic factors in organ-specific autoimmune diseases induced by manipulating the thymus or T cells, and not self-antigens. *Rev. Immunogenet. 2:147.*

American Journal of Pathology, Vol. 167, No. 4, October 2005

Immunology and Infectious Diseases

Analysis of *in Vivo* Role of α-Fodrin Autoantigen in Primary Sjögren's Syndrome

Katsushi Miyazaki,*† Noriaki Takeda,† Naozumi Ishimaru,* Fumie Omotehara,* Rieko Arakaki,* and Yoshio Hayashi*

From the Department of Pathology, Tokushima University School of Dentistry, Tokushima; and the Department of Otolaryngology,† The University of Tokushima, School of Medicine, Tokushima, Japan*

The α-fodrin N-terminal portion (AFN) autoantigen mediates *in vivo* immunoregulation of autoimmune responses in primary Sjögren's syndrome (SS). We further examined this process and found that cleavage products of AFN were frequently detected in the salivary gland duct cells of SS patients. In *in vitro* studies using human salivary gland HSY cells, anti-Fas-induced apoptosis resulted in specific cleavage of α-fodrin into the 120-kd fragment, in association of α-fodrin with μ-calpain, and activation of caspase 3. Significant proliferative responses against AFN autoantigen were observed in the peripheral blood mononuclear cells (PBMCs) from SS patients with higher pathological score (grade 4) and with short duration from onset (within 5 years). *In vivo* roles of AFN peptides were investigated using PBMCs from patients with SS, systemic lupus erythematosus, and rheumatoid arthritis. Significant proliferative T-cell responses of PBMCs to AFN peptide were detected in SS but not in systemic lupus erythematosus or rheumatoid arthritis. AFN peptide induced Th1-immune responses and accelerated down-regulation of Fas-mediated T-cell apoptosis in SS. Our data further elucidate the *in vivo* role of AFN autoantigen on the development of SS and suggest that the AFN autoantigen is a novel participant in peripheral tolerance. (Am J Pathol 2005, 167:1051–1059)*

Organ-specific autoimmune diseases are characterized by tissue destruction and functional decline due to autoreactive T cells that escape self-tolerance.[1,2] Primary Sjögren's syndrome (SS) is an autoimmune disorder characterized by lymphocytic infiltrates and destruction of the salivary and lacrimal glands, and systemic production of autoantibodies to the ribonucleoprotein particles SS-A/Ro and SS-B/La.[3–5] SS is a T-cell-mediated autoimmune disease, and autoreactive T cells bearing CD4 molecule may recognize unknown self antigen-triggering autoimmunity in the salivary and lacrimal glands, leading to clinical symptoms of dryness of the mouth and eyes (sicca syndrome).[6,7] Accumulated evidence suggest an important role of apoptosis in disease pathogenesis of SS.[8] Previously we have identified a 120-kd α-fodrin autoantigen in the pathogenesis of primary SS,[9] but the role of autoantigen that render *in vivo* immunoregulation remains unclear.

Although an important role for T cells on the development of organ-specific autoimmune disease has been argued, it is not known whether disease is initiated by a restrained inflammatory reaction to an organ-specific autoantigen. Autoreactive T cells generally respond to a limited number of immunodominant epitopes in self-antigenic proteins including myelin basic protein, thyroglobulin, and glutamic acid decarboxylase.[10–12] α-Fodrin is a ubiquitous, heterodimeric calmodulin-binding protein[13] found to be cleaved by calcium-activated protease (calpain) in apoptotic T cells, and by calpain and caspase family cysteine proteases[14] in anti-Fas-stimulated Jurkat cells and/or neuronal apoptosis.[15–17] Previous reports have demonstrated evidence that caspase 3 is required for α-fodrin cleavage during apoptosis.[18–20] In Jurkat cells, caspase 3-like proteases have been reported to cleave α-fodrin and poly (ADP-ribose) polymerase but with differential sensitivity to the caspase 3 inhibitor, DEVD-fmk.[20] In neuroblastoma cells, treatment with staurosporin induced cleavage of α-fodrin at both caspase 3 and calpain cleavage sites.[21] Therefore, we speculate that an increase in enzymatic activity of apoptotic proteases is involved in the progression of α-fodrin proteolysis during apoptosis of human salivary gland cells. In this study, we analyzed Fas-mediated apoptosis in SS

Supported in part by the Ministry of Education, Science, and Culture of Japan (grants-in-aid for scientific research nos. 12307040 and 12557022).

Accepted for publication July 5, 2005.

Address reprint requests to Yoshio Hayashi, Department of Pathology, Tokushima University School of Dentistry, 3 Kuramotocho, Tokushima 770, Japan. E-mail: hayashi@dent.tokushima-u.ac.jp.

salivary glands, and the *in vivo* role of the autoantigen for T-cell response, cytokine production, and peripheral tolerance.

Materials and Methods

Patients with Autoimmune Diseases

Peripheral blood samples from 18 patients with primary SS, 6 systemic lupus erythematosus (SLE), and 5 rheumatoid arthritis (RA), and from age-matched healthy donors (n = 18) were obtained from the Tokushima University Hospital, Tokushima, Japan. SLE and RA patients were diagnosed based on American College of Rheumatology criteria.[22,23] All patients with SS were female, had documented xerostomia and keratoconjunctivitis sicca, and fulfilled San Diego criteria for the diagnosis of SS.[3] Patients with secondary SS were carefully excluded. All patients with SS had focus scores of greater than 2 in their lip biopsy and all tested positive for autoantibodies against Ro, and 15 of 18 SS patients had autoantibodies against 120-kd α-fodrin by Western blotting. Analysis was performed under the certification of the ethics board of Tokushima University Hospital.

Immunohistology

Immunohistology was performed on freshly frozen sections (4 μm in thickness) by the biotin-avidin immunoperoxidase method using ABC reagent (Vector Laboratories, Burlingame, CA). Briefly, freshly frozen sections were fixed in acetone for 10 minutes, rinsed in phosphate-buffered saline (PBS, pH 7.2), and incubated with an appropriate blocking reagent (Vector Laboratories) for 20 minutes. They were incubated for 1 hour with biotinylated mouse monoclonal antibodies (mAbs) to CD4, CD8, L26(CD20) (BD Bioscience, San Jose, CA), and to Fas and FasL (BD PharMingen, San Diego, CA). To detect the cleavage product of α-fodrin, polyclonal rabbit Abs raised against the synthetic peptide to the purified 120-kd antigen corresponding to the identified 20 amino acid residues (RQKLEDSYRFQFFQRDAEEL) were developed and used.[9] Isotype-matched sera were used as controls, respectively.

Production of Recombinant α-Fodrin

Recombinant α-fodrin N-terminus (AFN) protein (JS-1), the cDNA encoding human α-fodrin (JS-1:1,1784 bp)[9] was constructed by inserting cDNA into the *Eco*RI site of pGEX-2T. Glutathione *S*-transferase fusion protein was expressed and purified using a glutathione *S*-transferase gene fusion system (Amersham Bioscience, Piscataway, NJ).

Synthetic Peptides

AFN peptides identical to JS-1 region were synthesized using tent-butoxycarbonyl chemistry on a model 430A peptide synthesizer (Applied Biosystems, Foster City, CA). A total of 45 synthetic peptides that were designed to be 20-amino acid residues in length, overlapping by five-amino acid residues were generated. As control peptide, laminin fragment peptide 929-933 (Sigma Chemical Co., St. Louis, MO) was used.

Proliferative T-Cell Response

Freshly isolated peripheral blood mononuclear cells (PBMCs) from SS patients and age-matched controls were assayed. When necessary, isolated $CD4^+$ and $CD8^+$ T cells from PBMCs using magnetic beads (Dynal, Oslo, Norway) were assayed. Single cell suspensions were cultured in 96-well flat-bottom microtiter plates (5×10^5 cells/well) in RPMI 1640 containing 10% fetal calf serum, penicillin/streptomycin, and β-mercaptoethanol. Cells were cultured with 10 μg/ml JS-1 protein, 10 μg/ml AFN peptide, and 2.0 μg/ml Con A (EY Laboratories, San Mateo, CA). To confirm the immunoreactivity with the AFN protein (JS-1), 2×10^5 $CD4^+$ and $CD8^+$ T cells from PBMCs of SS patients and controls were co-cultured with irradiated T-cell-depleted PBMCs as antigen-presenting cells, and stimulated with 0 to 20 μg/ml JS-1 for 72 hours. During the last 8 hours of the 72-hour culture period, 1 μCi of [^{3}H]thymidine was added per well, and the incorporated radioactivity was determined using an automated β liquid scintillation counter.

Flow Cytometric Analysis

For analysis of intracellular cytokines, monensin (Wako Pure Chemical, Osaka, Japan) was added at 2 μmol/L to isolated PBMCs (10^6/ml), and 2 hours later the cells were collected, labeled with anti-CD4-PE (BD PharMingen), fixed with 4% paraformaldehyde for 10 minutes at 4°C, and then permeabilized with 0.1% saponin in PBS at room temperature for 10 minutes. Cells were incubated with anti-interleukin (IL)-2-fluorescein isothiocyanate (FITC) (8 μg/ml; BD PharMingen), anti-IL-4-FITC (5 μg/ml; BD PharMingen), and anti-interferon (IFN)-γ-FITC (1 μg/ml; BD PharMingen), respectively, and analyzed on a EPICS flow cytometer (Beckman Coulter, Miami, FL). For analysis of Fas and FasL expression, isolated PBMCs from SS patients when pulsed with AFN peptide (10 μg/ml) were assayed by flow cytometry gated on $CD4^+$ T cells, using anti-Fas and anti-FasL mAb (BD PharMingen). Mean fluorescence intensity was calculated using the fluorescence intensity of staining for mAbs to Fas or FasL and isotype-matched control measured by flow cytometry. Apoptotic cells were detected by flow cytometry with an EPICS (Beckman Coulter) using the Annexin V-FITC apoptosis detection kit (Genzyme, Cambridge, MA).

Cell Culture and Induction of Apoptosis

Human parotid salivary gland HSY cells[24] were grown in Dulbecco's modified Eagle's medium supplemented with 10% heat-inactivated fetal calf serum, 100 U/ml penicillin, and 100 μg/ml streptomycin in a humidified atmosphere

of 5% CO_2 in air at 37°C. The cells were maintained in a logarithmic growth phase by routine passage every 2 to 3 days. Apoptosis was induced in HSY cells by anti-Fas mAb (clone CH-11; Medical and Biological Laboratories. Co., Ltd., Nagoya, Japan).

Western Blot Analysis

For detection of a cleavage product of α-fodrin, Western blot analysis was performed with anti-α-fodrin mAb (Affiniti, Mamhead, UK). To detect the apoptotic proteases *in vitro*, Western blot analysis was performed using mouse mAbs to μ-calpain (clone 9; Chemicon Int., Temecula, CA) specific for catalytic subunit (80 kd), calpastatin (clone 1F7E3D10; Calbiochem, San Diego, CA) specific for amino acids 543 to 673 encoding domain IV (150, 125, 90, and 70 kd), and caspase 3 (3G2; Transduction Laboratories, Lexington, KY) specific for amino acids 28 to 44 encoding large subunit (17/19 kd). The cells were homogenized in 20 mmol/L Tris-HCl buffer (pH 7.4) containing 5 mmol/L ethylene diamine tetraacetic acid, 10 μl/ml protease inhibitor cocktail (Sigma Chemical Co.) and 0.2% Triton X-100. After centrifugation for 20 minutes at 12,000 × *g* at 4°C, supernatant was extracted and used for cytoplasmic protein. Pellets were homogenized in 20 mmol/L Tris-HCl buffer containing 2% Triton X-100. Protein binding was visualized with ECL Western blotting reagent (Amersham Bioscience). Protease inhibitors included leupeptin, E64, pepstatin (Wako Pure Chemicals), calpain inhibitor peptide (Sigma Chemical Co.), and caspase inhibitors [Ac-YVAD-CHO (ICN, Costa Mesa, CA); Z-VAD-fmk (ICN)].

Sequential Activation of Caspase-Like Proteases

The caspase 3-like activity in anti-Fas mAb-treated HSY cell extracts was determined using fluorescent substrate.[25] Cell lysates were diluted with 0.5 ml of standard buffer, and incubated at 30°C for 30 minutes with 1 μmol/L fluorescent substrate. The specific inhibitor for caspase 3 (Z-DEVD-fmk) was added to the reaction mixture at a concentration of 1 μmol/L. Specific caspase 3-like activity was determined by subtracting the values obtained in the presence of inhibitors. The fluorescent substrate, MOCAc-DEVD (dnp)-NH_2 was custom-synthesized at the Peptide Institute (Osaka, Japan). The fluorescence of the cleaved substrates was determined using a spectrofluorometer set at an excitation wavelength of 328 nm and an emission wavelength of 393 nm.

Cell Transfection

cDNAs for full-length caspase 3 and μ-calpain obtained by polymerase chain reaction were subcloned into the pCRII vector (Invitrogen Co., Carlsbad, CA). All constructs were confirmed by DNA sequencing. For expression experiments, DNA fragments were subcloned into pcDNA3.1 expression vector (Invitrogen Co.). HSY cells were transfected with the pcDNA3.1 expression vectors using the Lipofectamine reagent according to the manufacturer's instruction (Invitrogen Co.). The cells were transfected with the individual plasmid DNA and the total amount of DNA transfected was adjusted to 10 μg with pcDNA3.1 for each 100-mm dish or 3 μg for each 60-mm dish. After a 5-hour incubation with the DNA/lipid mixture, the cells were washed with PBS before replenishing with growth media. The cells were harvested 24 hours after transfection and lysed in Tris-HCl buffer.

Results

Involvement of Apoptotic Cascade in SS Salivary Glands

Immunohistochemical analysis revealed that a majority of infiltrating cells were $CD4^+$, and that a small number of $CD8^+$ cells were present in the SS salivary glands. $L26^+$ B cells were sporadically present in the inflammatory lesions (data not shown). Shown in Figure 1, A and B, are photomicrographs taken from representative data. Immunofluorescence analysis revealed that a large number of infiltrating lymphoid cells bear FasL in SS salivary glands (Figure 1C), and epithelial duct cells stained positively with Fas on their cell surface (Figure 1D). Some acinar cells were stained negligibly positive with both anti-FasL and anti-Fas antibodies, but most acinar cells were negative. Immunofluorescence analysis using polyclonal Ab against synthetic 120-kd α-fodrin[9] demonstrated that a cleavage product of α-fodrin was present in epithelial duct cells of the labial salivary gland biopsies from SS patients, but not in control glands (Figure 1, E and F). Western blot analysis confirmed the same results (Figure 1G), indicating that a cleavage product of 120-kd α-fodrin is present in the diseased glands with SS.

In Vitro *Cleavage of α-Fodrin Induced by Apoptotic Stimuli*

We examined the *in vitro* cleavage of α-fodrin using HSY and Jurkat cells induced by anti-Fas mAb (ranging from 1 to 1000 ng/ml^{-1}) apoptotic stimuli. Anti-Fas (CH-11)-stimulated apoptosis in HSY cells was confirmed by flow cytometric analysis using an apoptosis detection kit as well as in Jurkat cells (Figure 2A). Western blot analysis demonstrated that the 240-kd α-fodrin on apoptotic HSY cells was cleaved into smaller 120-kd fragments in dose-dependent manner of anti-Fas mAb (Figure 2B). We next examined whether α-fodrin cleavage into the 120-kd fragment on apoptotic HSY cells could be blocked by preincubation with specific protease inhibitors. In apoptotic HSY cells, a combination of calpain inhibitor peptide and caspase inhibitor (Z-VAD-fmk) entirely blocked the formation of 120-kd α-fodrin, whereas calpain inhibitor peptide alone could not block 120-kd formation (Figure 2C). Caspase inhibitor alone could block considerably 120-kd formation. Cysteine protease inhibitors (E64), serine pro-

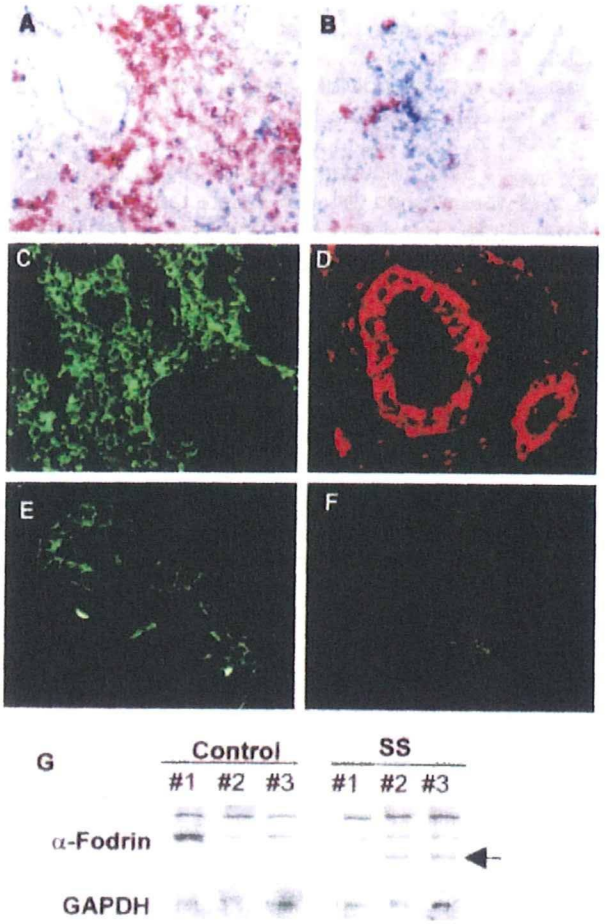

Figure 1. Representative immunohistological features in the labial gland biopsies. A majority of infiltrating cells were $CD4^+$ (**A**), and a small number of $CD8^+$ T cells (**B**) were present in the SS salivary glands. Five samples were examined. Immunofluorescence analysis revealed that the majority of tissue-infiltrating lymphoid cells bear FasL (**C**), and epithelial duct cells stained positively with Fas on their cell surface (**D**) in SS salivary glands. Isotype-matched controls were stained negatively. Six samples for each were examined. A cleavage product of 120-kd α-fodrin was present exclusively in epithelial duct cells of the SS salivary glands (**E**), but not in control salivary glands (**F**). Six samples for each were examined. Detection of a cleavage product of 120-kd α-fodrin in the labial salivary gland biopsies with SS (no. 1, no. 2, and no. 3), but not in control individuals (no. 1, no. 2, and no. 3) on Western blotting (**G**). Eight samples for each were examined.

tease inhibitor (leupeptin), and acidic protease inhibitor (pepstatin) had no effect on 120-kd α-fodrin cleavage.

Calpain and Caspase Mediated α-Fodrin Cleavage

We investigated whether cysteine proteases are involved in α-fodrin cleavage on apoptotic HSY cells. We found a constitutive expression of μ-calpain, and its time-dependent increase in anti-Fas-stimulated HSY cells (Figure 3A). Of note is that abundant calpastatin activity is shown to be constitutively expressed more than calpain expression, and a time-dependent decrease of calpastatin expression was observed in apoptotic HSY cells, not in Jurkat cells (Figure 3A). It can be speculated that μ-calpain activity could be considerably affected by endogenous calpastatin during apoptosis in HSY cells. We confirmed a time-dependent increase in the active form of μ-calpain in apoptotic HSY cells (Figure 3A). Anti-Fas-stimulated HSY cells were positive for mAbs to caspase 3 in association with apoptosis (Figure 3B). Moreover, the caspase 3-like activities in anti-Fas Ab-stimulated HSY cell extracts were determined using fluorescent substrates (Figure 3B).[25] To confirm the role of caspase 3 and μ-calpain proteins in induction of α-fodrin cleavage, full-length caspase 3 and μ-calpain cDNAs were transiently overexpressed in HSY cells, and cleavage product of 120-kd α-fodrin was examined by anti-α-fodrin Ab. Analysis of lysates from caspase 3 and μ-calpain cDNA co-transfected cells with Western blotting revealed a significant increase (approximately fivefold to sevenfold) of 120-kd α-fodrin in the level of expression of caspase 3 or μ-calpain in cells transfected with respective cDNA (Figure 3C).

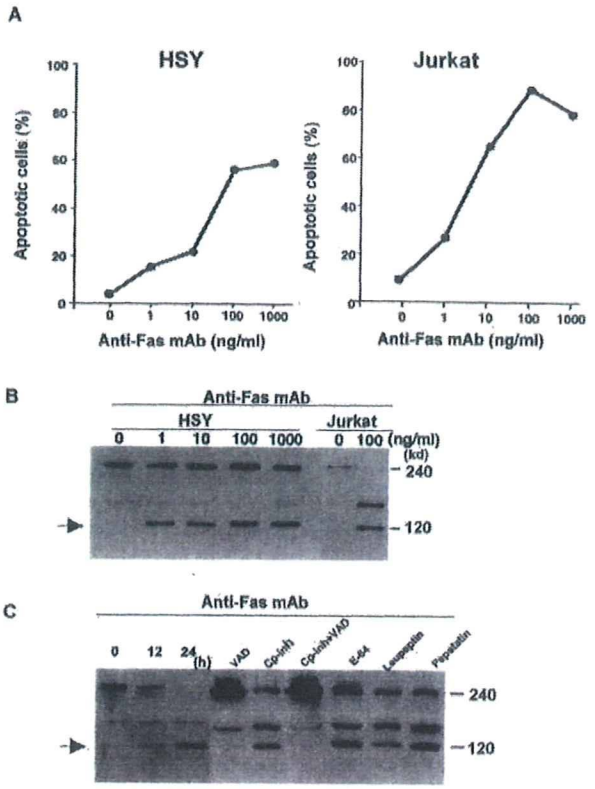

Figure 2. Anti-Fas-induced apoptosis in HSY and Jurkat cells. **A:** The HSY and Jurkat cell apoptosis induced by anti-Fas mAb (CH-11) stimulation was determined by flow cytometry of DNA content of nuclei with PI and annexin V. **B:** Western blot analysis demonstrated 120-kd α-fodrin in apoptotic HSY and Jurkat cells in a dose-dependent manner. **C:** Effects of protease inhibitors on α-fodrin cleavage in apoptotic HSY cells. Proteolytic cleavage of α-fodrin to 120 kd in Fas-stimulated HSY cells is blocked by a combination of a calpain inhibitor peptide and caspase inhibitors (Z-VAD-fmk), but not by E64, leupeptin, and lepstatin. Calpain inhibitor peptide alone could not inhibit the 120-kd α-fodrin formation.

In Vivo *Role of α-Fodrin in SS Patients*

To confirm the immunoreactivity with the AFN protein (JS-1), $CD4^+$ and $CD8^+$ T cells were isolated from PBMCs of SS patients (n = 3) and controls (n = 2), and were co-cultured with irradiated T-cell-depleted

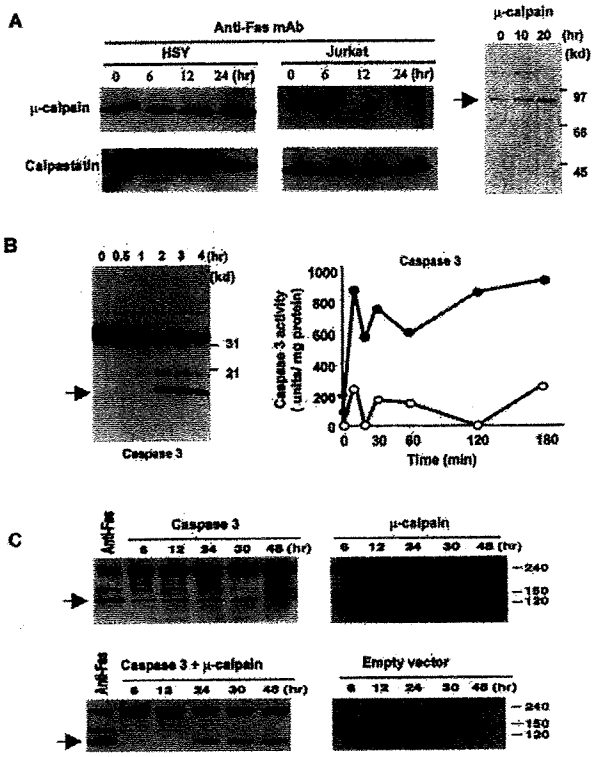

Figure 3. Detection of cysteine proteases in anti-Fas-induced apoptotic HSY cells. Western blot analysis of μ-calpain, and calpastatin in apoptotic HSY and Jurkat cells stimulated with anti-Fas Ab (CH-11). A constitutive expression of μ-calpain, and its time-dependent increase were observed in anti-Fas-stimulated HSY cells. Calpastatin activity is shown to be constitutively expressed,more than calpain expression and a time-dependent decrease of calpastatin expression was observed in apoptotic HSY cells, not in Jurkat cells. **A:** Western blot analysis of the active form of μ-calpain in apoptotic HSY cells stimulated with anti-Fas mAb (CH-11). **B:** Western blot analysis showing a time-dependent increase in caspase 3 and sequential activation of caspase 3-like protease in anti-Fas-induced apoptotic HSY cells. The caspase 3-like activity in the lysates (100 mg protein) (**filled circle**) or in the presence of 50 mmol/L MOCAc-DEVD-NH2 (**open circle**) was determined using fluorescent substrates in apoptotic HSY cells. One unit corresponds to the activity that cleaves 1 pmol of the respective fluorescent substrate at 30°C in 30 minutes. **C:** Detection of cleavage product of 120-kd α-fodrin in co-transfected HSY cells overexpressed with full-length caspase 3 and μ-calpain cDNAs. Analysis of lysates from caspase 3 and μ-calpain cDNA co-transfected cells revealed a fivefold to sevenfold increase of 120-kd α-fodrin in the level of expression of caspase 3 or μ-calpain in cells transfected with each construct.

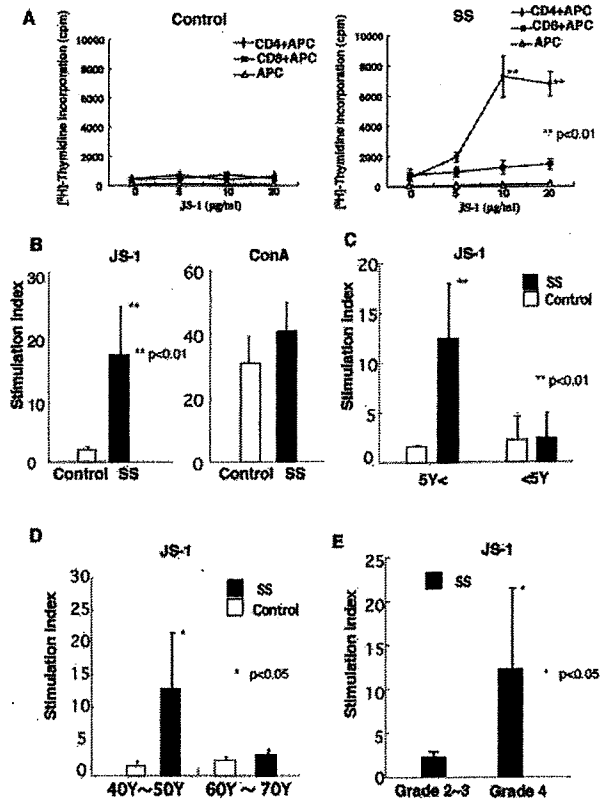

Figure 4. A: Significant proliferative $CD4^+$ T-cell responses, not $CD8^+$ T cells, to the AFN protein (JS-1) in the patients with primary SS ($n = 3$), not in age-matched control ($n = 2$) (**$P < 0.01$, Student's *t*-test). **B:** Significant proliferative responses (stimulation indices > 3) of PBMCs to the AFN protein (JS-1) in patients with primary SS ($n = 14$), not in age-matched control ($n = 11$) (**$P < 0.01$, Student's *t*-test). **C:** Proliferative responses to JS-1 of PBMCs from SS patients with short duration (within 5 years) from the onset of the disease ($n = 8$) were significantly higher than those with long duration (more than 5 years) ($n = 6$) (**$P < 0.01$, Student's *t*-test). **D:** Proliferative responses to JS-1 of PBMCs from younger SS patients (40 to 50 years of age) ($n = 8$) were significantly higher than those with older SS patients (60 to 70 years of age) ($n = 6$) (*$P < 0.05$, Student's *t*-test). **E:** Significant proliferative responses to JS-1 protein were observed in PBMCs from SS patients with higher pathological score ($n = 9$, grade 4) than those with lower score ($n = 5$, grade 2 or grade 3) (*$P < 0.05$, Student's *t*-test). All data are expressed as stimulation indices ± SEM.

PBMCs as antigen-presenting cells. Significant proliferative responses were observed in $CD4^+$ T cells from SS patients, not in $CD8^+$ T cells (Figure 4A). Moreover, it has been determined by flow cytometric analysis that the accumulated population in response to both AFN protein (JS-1) and AFN peptide among PBMCs of SS patients is $CD4^+$ T cell (data not shown). Then, we used PBMCs for the proliferation assay. We found proliferative T-cell responses (stimulation indices > 3) to the AFN protein (JS-1) using PBMCs from 14 of 18 patients with SS, not from age-matched healthy patients ($n = 11$) (Figure 4B). Proliferative responses to JS-1 of SS patients with short duration (within 5 years) from the onset of disease ($n = 8$) were significantly higher than those with long duration (longer than 5 years) ($n = 6$) (Figure 4C). Proliferative responses to JS-1 autoantigen with younger SS patients (40 to 50 years of age) ($n = 8$) were significantly higher than those with older SS patients (60 to 70 years of age) ($n = 6$) (Figure 4D). Significant proliferative responses to JS-1 protein were observed in PBMCs from SS patients with higher pathological score ($n = 9$, grade 4) than those with lower score ($n = 5$, grade 2 or grade 3) (Figure 4E). Synthetic peptides of AFN were generated, and immunoregulatory roles were investigated using PBMCs from patients with SS, compared with SLE and RA. Significant proliferative T-cell responses to AFN peptide were detected in PBMCs from 9 of 18 patients with SS, but not with SLE, RA, and healthy controls (Figure 5). We next analyzed intracellular cytokines using isolated PBMCs (10^6/ml). $CD4^+$ T cells from PBMCs with SS patients induce Th1 cytokine (IL-2, IFN-γ) when pulsed with AFN peptide (10 μg/ml) (Figure 6A), not with control laminin fragment peptide (10 μg/ml). We observed a significant decrease in both $CD4^+$ Fas^+ T and $CD4^+$ $FasL^+$ T cells in SS patients,

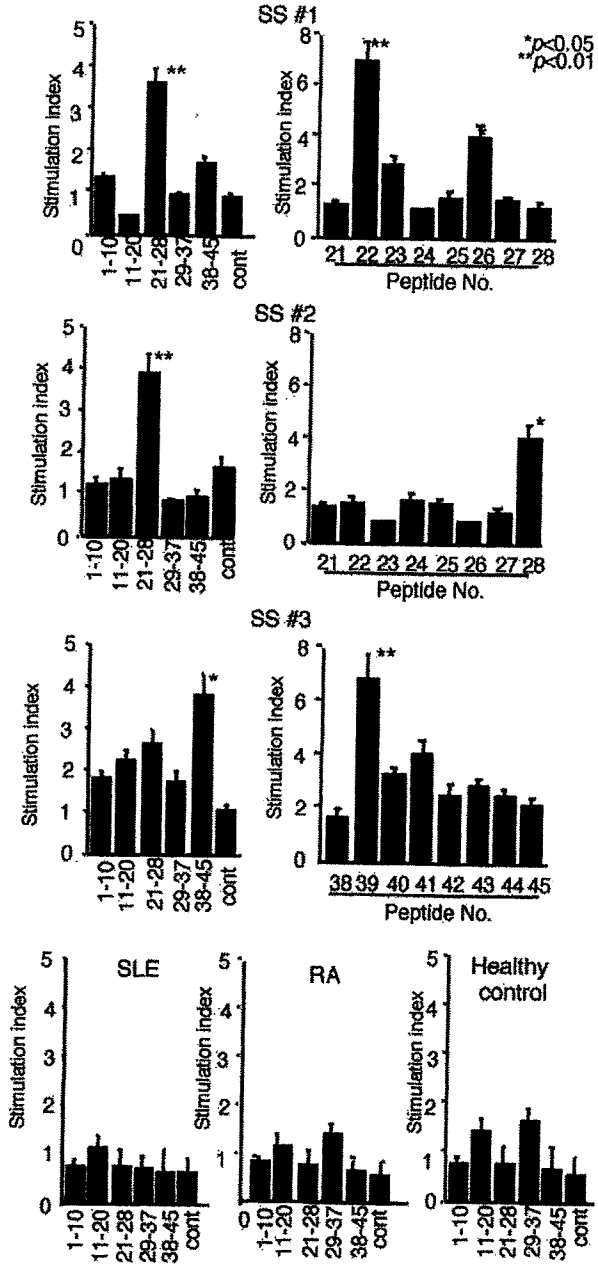

Figure 5. Significant proliferative responses of PBMCs were seen with AFN peptide in the patients with primary SS. Nine of eighteen SS patients examined reacted significantly with single AFN peptide, but not in SLE ($n = 6$), RA ($n = 5$), and age-matched healthy controls ($n = 6$). Representative profiles in three different patients with SS (SS 1, SS 2, SS 3) indicate significant proliferative responses with peptide mixture and individual peptide of p22, p26, p28, and p39 ($^*P < 0.05$, $^{**}P < 0.01$; Student's *t*-test), but not with laminin fragment peptide 929-933 as control antigen. The results are expressed as stimulation indices ± SEM.

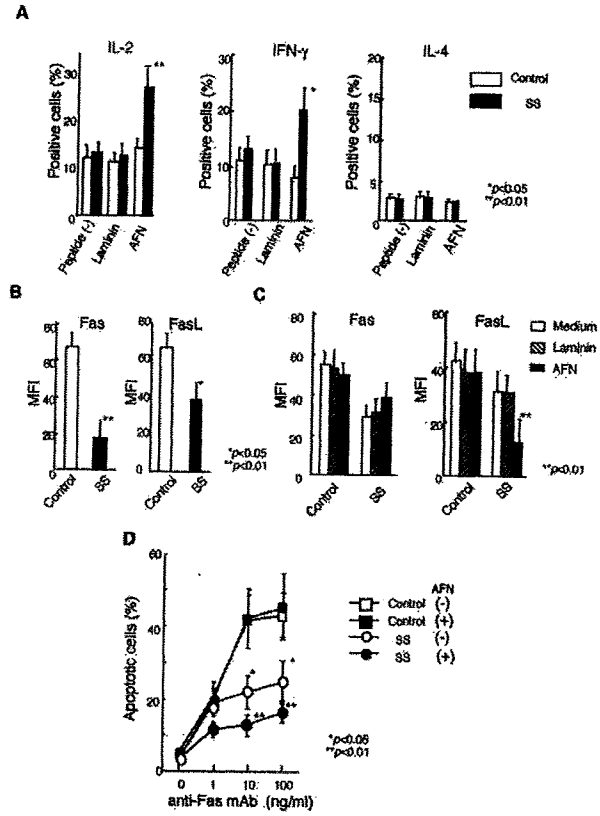

Figure 6. Cytokine profile and Fas-mediated apoptosis in $CD4^+$ T cells from SS patients. **A:** $CD4^+$ T cells from PBMCs with SS patients induce Th1 cytokine (IL-2, IFN-γ), not Th2 cytokine (IL-4) when pulsed with AFN peptide (10 μg/ml) by flow cytometric analysis ($^*P < 0.05$, $^{**}P < 0.01$; Student's *t*-test). Laminin fragment peptide 929-933 (10 μg/ml) was used as control. Five SS patients were analyzed. **B:** Significant decrease in both Fas^+ and $FasL^+$ expression in $CD4^+$ T cells from SS patients, compared with healthy controls ($^*P < 0.05$, $^{**}P < 0.01$; Student's *t*-test). Five SS patients and four healthy controls were analyzed. **C:** AFN peptide-pulsed $CD4^+$ T cells showing significant low intensity of FasL expression, not Fas expression, in SS patients ($^{**}P < 0.01$, Student's *t*-test). MFI (mean fluorescence intensity) indicates the fluorescence intensity of positively stained sample/the fluorescence intensity of its isotype control. Mean fluorescence intensity was calculated using the fluorescence intensity of staining for mAbs to Fas or FasL and isotype-matched control measured by flow cytometry. Five SS patients and four healthy controls were analyzed. **D:** Anti-Fas mAb-stimulated apoptosis showed significant decrease in $CD4^+$ T cells from SS patients than those from healthy control. Moreover, anti-Fas mAb-stimulated apoptosis decreased more significantly in $CD4^+$ T cells from SS patients pulsed with AFN peptide, than those with nonpulsed cells ($^*P < 0.05$, $^{**}P < 0.01$; Student's *t*-test). Five SS patients and four healthy controls were analyzed.

compared with healthy controls (Figure 6B). Moreover, it was demonstrated that AFN peptide-pulsed $CD4^+$ T cells showed a significant low intensity of FasL expression, not Fas expression (Figure 6C). Anti-Fas mAb-stimulated apoptosis showed a significant decrease in $CD4^+$ T cells from SS patients than those from healthy control (Figure 6D). When pulsed with AFN peptide, anti-Fas mAb-stimulated apoptosis decreased more significantly in $CD4^+$ T cells from SS patients.

Discussion

Cleavage of certain autoantigens during apoptosis may reveal immunocryptic epitopes that could potentially induce autoimmune responses in systemic autoimmune diseases.[26,27] We reported previously that a cleavage product of 120-kd α-fodrin may be an important autoantigen on the development of primary SS, and anti-120-kd α-fodrin antibodies have been frequently detected in sera from patients.[9] Although several candidate autoantigens besides α-fodrin have

been reported in SS,[28–30] the pathogenic roles of the autoantigens in initiation and progression of SS are still unclear.

The specificity of cytotoxic T-lymphocyte function has been an important issue of organ-specific autoimmune response, but little is known about the events triggering T-cell invasion of the target organs in prelude to organ-specific autoimmune diseases. In insulin-dependent diabetes mellitus, the role of environmental factors,[31,32] the nature of the initiating T cell,[33,34] and the identity of the inciting antigen(s)[35] have all been vigorously debated. When we analyzed the mechanisms of α-fodrin cleavage in the SS salivary glands, infiltrating mononuclear cells bear a large proportion of $CD4^+$ and Fas ligand (FasL), and the salivary gland duct cells constitutively possess Fas. In particular, cleavage products of 120-kd α-fodrin were frequently detected in the salivary gland duct cells with SS, but not in control salivary glands. Thus, we provided evidence suggesting that Fas-mediated apoptosis may be involved, in part, in *in vivo* α-fodrin cleavage in SS salivary glands. Moreover, it has been suggested that α-fodrin cleavage triggered by estrogen deficiency plays an important role in the development of autoimmune exocrinopathy in SS. Experimental studies of ours demonstrated a significant apoptosis associated with α-fodrin cleavage in the salivary gland cells of estrogen-deficient healthy C56BL/6(B6) mice, and inflammatory lesions developed exclusively in the salivary and lacrimal gland after the adoptive transfer with α-fodrin-reactive T cells in both ovariectomized (Ovx)-B6 and Ovx-SCID mice.[36] Reduction of the intact form of α-fodrin in the affected glands suggests that elicitation of autoreactivity against α-fodrin could be the primary pathogenetic process that leads to tissue destruction. However, based on the fact that α-fodrin is a ubiquitous protein, and that the tissue destruction is confined to exocrine organs, it might be more reasonable to speculate that other undetermined tissue-specific target antigens in exocrine glands could be the primary target of the disease process mediated by pathogenic T cells. Nevertheless, production of autoantibodies and proliferative T-cell responses against cleavage product of α-fodrin, which does not take place under physiological conditions, might be an important clue that could shed light on the novel mechanisms by which tissue-specific apoptosis contributes to the disease development.

It has been reported that calpain is overactivated in autoimmune conditions, and subsequent tissue destruction.[37,38] Moreover, the cascade of caspases is a critical component of the cell death pathway,[39–41] and a few proteins have been found to be cleaved during apoptosis. These include poly (ADP-ribose) polymerase, a small U1 nuclear ribonucleoprotein, and α-fodrin, which were subsequently identified as substrates for caspases.[27,42] Anti-Fas-induced cleavage of α-fodrin in Jurkat cells produces a predominant 120-kd fragment, and the 120-kd fragment is consistent with a previously reported caspase 3-mediated DETD cleavage site within the protein.[20,21] Although the relevance of cleavage of structural proteins, including gelsolin, actins, lamins, and fodrins, is easily conceivable,[43] the functional importance is not yet clear. Our data provide evidence that α-fodrin in human HSY cells is cleaved into 120-kd fragment by apoptotic proteases including calpain and caspases. When we investigated whether cysteine proteases are involved in α-fodrin cleavage, anti-Fas-treated HSY cells were positive for mAb to μ-calpain, and caspase 3 in association with apoptosis. However, we demonstrated here that calpastatin, an endogenous inhibitor of calpain, was shown to be constitutively expressed, speculating that μ-calpain activity could be considerably affected during apoptosis in HSY cells. A combination of calpain inhibitor peptide and caspase inhibitors (Z-VAD-fmk) entirely blocked the formation of 120-kd α-fodrin. When both full-length caspase 3 and μ-calpain cDNAs were transiently overexpressed in HSY cells, a cleavage product of 120-kd α-fodrin was abundantly identified than the level of expression of caspase 3 or μ-calpain in cells transfected with each construct. These data suggest that both μ-calpain and caspase 3 are required for specific α-fodrin proteolysis into the 120-kd fragment in human salivary gland cells with SS.

In this study, we detected proliferative T-cell responses to AFN protein (JS-1) of SS patients with short duration (within 5 years) from the onset of the disease were significantly higher than those with long duration (more than 5 years). Proliferative responses to autoantigen with younger SS patients (40 to 50 years of age) were significantly higher than those with older SS patients (60 to 70 years of age). Moreover, significant proliferative responses to AFN protein were observed in SS patients with higher pathological score (grade 4) than those with lower score (grade 2 or grade 3). These data are suggestive of clinicopathological usefulness of AFN immunoreactivity with SS patients for disease severity in addition to diagnostic significance. Because we have detected proliferative response to AFN peptides using PBMCs from SS patients, it is feasible for the future possibility that a peptide analogue of AFN could be used as a therapeutic agent. On the other hand, Fas/FasL interaction down-regulates the immune response by inducing apoptosis because activated lymphocytes express both Fas and FasL.[44] $CD4^+$ T cells from PBMCs with SS patients induce Th1 cytokine (IL-2, IFN-γ) when pulsed with each peptide, suggesting that the autoantigen peptide may play an important role in Th1/Th2 balance *in vivo*. Moreover, AFN peptide-pulsed $CD4^+$ T cells down-regulate Fas-mediated apoptosis. Although antigen-induced T-cell death is known to be regulated by CD4 expression,[45] molecular mechanisms responsible for T-cell death should be further elucidated. Our previous findings support the notion that Fas-mediated T-cell death is down-regulated by autoantigen stimulation in the murine SS model.[46] Here we demonstrated that AFN peptide stimulation results in a significant decrease in anti-Fas-induced $CD4^+$ T-cell apoptosis. However, it remains unclear whether T cells specific for endogenous

epitopes play a significant pathological role in tissue damage during the clinical episodes.

Taken together, our results suggest that 120-kd α-fodrin, the apoptosis-associated breakdown product, may have an important role in the development of SS, and that the autoantigen is a novel participant in the regulation of Th1/Th2 balance and peripheral tolerance.

References

1. Gianani R, Satventnick N: Virus, cytokine, antigens, and autoimmunity. Proc Natl Acad Sci USA 1996, 93:2257–2259
2. Feldmann M, Bennan FM, Maini RN: Rheumatoid arthritis. Cell 1996, 85:307–310
3. Fox RI, Robinson CA, Curd JG, Kozin F, Howell FV: Sjögren's syndrome. Proposed criteria for classification. Arthritis Rheum 1986, 29:577–585
4. Chan EK, Hamel JC, Buyon JP, Tan ET: Molecular definition and sequence motifs of the 52-kD component of human SS-A/Ro autoantigen. J Clin Invest 1991, 87:68–76
5. Kruize AA, Smeenk RJT, Kater L: Diagnostic criteria and immunopathogenesis of Sjögren's syndrome. Immunol Today 1995, 16:557–559
6. Fox RI, Stern M, Michelson P: Update in Sjögren's syndrome. Curr Opin Rheumatol 2000, 12:391–398
7. Manoussakis MN, Moutsopoulos HM: Sjögren's syndrome: current concepts. Adv Intern Med 2001, 47:191–217
8. Humpherys-Beher MG, Peck AB, Dang H, Talal N: The role of apoptosis in the initiation of the autoimmune response in Sjögren's syndrome. Clin Exp Immunol 1999, 116:383–387
9. Haneji N, Nakamura T, Takio K, Yanagi K, Higashiyama H, Saito I, Noji S, Sugino H, Hayashi Y: Identification of α-fodrin as a candidate autoantigen in primary Sjögren's syndrome. Science 1997, 276:604–607
10. Harrington CJ, Paez A, Hunkapiller T, Mannikko V, Brabb T, Ahearn M, Beeson C, Goverman J: Differential tolerance is induced in T cells recognizing distinct epitopes of myelin basic protein. Immunity 1998, 8:571–580
11. Dai Y, Carayanniotis KA, Eliades P, Lymberi P, Shepherd P, Kong Y, Carayanniotis G: Enhancing or suppressive effects of antibodies on processing of a pathogenic T cell epitope in thyroglobulin. J Immunol 1999, 162:6987–6992
12. Hoglund P, Mintern J, Waltzinger C, Heath W, Benoist C, Mathis D: Initiation of autoimmune diabetes by developmentally regulated presentation of islet cell antigens in the pancreatic lymph nodes. J Exp Med 1999, 189:331–339
13. Leto TL, Pleasic S, Forget BG, Benz Jr EJ, Marchesi VT: Characterization of the calmodulin-binding site of nonerythroid α-spectrin. J Biol Chem 1989, 264:5826–5830
14. Alnemri ES, Livingstin DJ, Nicholson DW, Salvensen G, Thornberry NA, Wong WW, Yuan J: Human ICE/CED-3 protease nomenclature. Cell 1996, 87:171
15. Martin SD, O'Brien GA, Nishioka WK, McGahon AJ, Mahboubi A, Saido TV, Green DR: Proteolysis of fodrin (non-erythroid spectrin) during apoptosis. J Biol Chem 1995, 270:6425–6428
16. Martin SD, Finucane DM, Amarante-Mendes GP, O'Brien GA, Green DR: Phosphatidylserine externalization during CD95-induced apoptosis of cells and cytoplasts requires ICE/CED-3 protease activity. J Biol Chem 1996, 271:28753–28756
17. Vanags DM, Pörn-Ares I, Coppolaa S, Burgess DH, Orrenius S: Protease involvement in fodrin cleavage and phosphatidylserine exposure in apoptosis. J Biol Chem 1996, 271:31075–31085
18. Nath R, Raser KJ, Stafford D, Hajimohammadreza I, Posner A, Allen H, Talanian RV, Yuen P, Gilbertsen RB, Wang KK:. Non-erythroid α-spectrin breakdown by calpain and interleukin 1β-converting-enzyme-like protease(s) in apoptotic cells: contributory roles of both protease families in neuronal apoptosis. Biochem J 1996, 319:683–690
19. Janicke RU, Sprengart ML, Porter AG: Caspase-3 is required for alpha-fodrin cleavage but dispensable for cleavage of other death substrates in apoptosis. J Biol Chem 1996, 273:15540–15545
20. Cryns VL, Bergeron L, Zhu H, Li H, Yuan J: Specific cleavage of alpha-fodrin during Fas- and tumor necrosis factor-induced apoptosis is mediated by an interleukin-1beta-converting enzyme/Ced-3 protease distinct from the poly(ADP-ribose) polymerase protease. J Biol Chem 1996, 271:31277–31282
21. Wang KW, Posmantur R, Nath R, McGinnis K, Whitton M, Talanian RV, Glantz, Marrow JS: Simultaneous degradation of alphaII- and betaII-spectrin by caspase 3 (CPP32) in apoptotic cells. J Biol Chem 1998, 273:22490–22497
22. Tan EM, Cohen AS, Fries JF, Masi AT, McShane DJ, Rothfield NF, Schaller JG, Talal N, Winchester RJ: The 1982 revised criteria for the classification of systemic lupus erythematosus. Arthritis Rheum 1982, 25:1271–1277
23. Arnett FC, Edworthy SM, Bloch DA, McShane DJ, Fries JF, Cooper NS, Healey LA, Kaplan SR, Liang MH, Luthra HS: The American Rheumatism Association 1987 revised criteria for the classification of rheumatoid arthritis. Arthritis Rheum 1988, 31:315–324
24. Hayashi Y, Yanagawa T, Yoshida H, Azuma M, Nishida T, Yura Y, Sato M: Expression of vasoactive intestinal polypeptide and amylase in a human parotid gland adenocarcinoma cell line in culture. J Natl Cancer Inst 1987, 79:1025–1037
25. Enari M, Talanian RV, Wong WW, Nagata S: Sequential activation of ICE-like and CPP32-like proteases during Fas-mediated apoptosis. Nature 1996, 380:723–726
26. Utz PJ, Hottelet M, Schur PH, Anderson P: Proteins phosphorylated during stress-induced apoptosis are common targets for autoantibody production in patients with systemic lupus erythematosus. J Exp Med 1997, 185:843–854
27. Casiano CA, Martin SJ, Green DR, Tan EM: Selective cleavage of nuclear autoantigens ensuring CD95 (Fas/APO-1)-mediated T cell apoptosis. J Exp Med 1996, 184:765–770
28. Robinson CP, Brayer J, Yamachika S, Esch TR, Peck AB, Stewart CA, Peen R, Jonsson R, Humphreys-Beher MG: Transfer of human serum IgG to nonobese diabetic $Ig\mu^{null}$ mice reveals a role for autoantibodies in the loss of secretory function of exocrine tissues in Sjögren's syndrome. Proc Natl Acad Sci USA 1998, 95:7538–7543
29. Kuwana M, Okano T, Ogawa Y, Kaburaki J, Kawakami Y: Autoantibodies to the amino terminal fragment of β-fodrin expressed in glandular epithelial cells in patients with Sjögren's syndrome. J Immunol 2001, 167:5449–5456
30. Winer S, Astsaturov I, Cheung R, Tsui H, Song A, Gaedigk R, Winer D, Sampson A, McKerlie C, Bookman A, Dosch HM: Primary Sjögren's syndrome and deficiency of ICA69. Lancet 2002, 360:1063–1069
31. Singh B, Prange S, Jevnikar AM: Protective and destructive effects of microbial infection in insulin-dependent diabetes mellitus. Semin Immunol 1998, 10:79–86
32. Wong FS, Janeway Jr CA: The role of CD4 and CD8 T cells in type I diabetes in the NOD mouse. Res Immunol 1997, 148:327–332
33. Wegmann DR: The immune response to islets in experimental diabetes and insulin-dependent diabetes mellitus. Curr Opin Immunol 1996, 8:860–864
34. Kay TW, Chaplin HL, Parker JL, Stephens LA, Thomas HE: $CD4^+$ and $CD8^+$ T lymphocytes: clarification of their pathogenic roles in diabetes in the NOD mouse. Res Immunol 1997, 148:320–327
35. Patel T, Gores GJ, Kaufmann SH: The role of proteases during apoptosis. FASEB J 1996, 10:587–597
36. Ishimaru N, Arakaki R, Watanabe M, Kobayashi M, Miyazaki K, Hayashi Y: Development of autoimmune exocrinopathy resembling Sjogren's syndrome in estrogen-deficient mice of healthy background. Am J Pathol 2003, 163:1481–1490
37. Menad H-A, el-Amine M: The calpain-calpastatin system in rheumatoid arthritis. Immunol Today 1996, 17:545–547
38. Mimori T, Suganuma K, Tanami Y, Nojima T, Matsumura M, Fujii T, Yoshizaka T, Suzuki K, Akizuki M: Autoantibodies to calpastatin (an endogenous inhibitor for calcium-dependent neutral protease, calpain) in systemic rheumatic diseases. Proc Natl Acad Sci USA 1995, 92:7267–7271
39. Holtzman DM, Deshmukh M: Caspases: a treatment target for neurodegenerative disease? Nat Med 1997, 3:954–955
40. Rudel T, Bokoch GM: Membrane and morphological changes in

apoptotic cells regulated by caspase-mediated activation of PAK2. Science 1997, 276:1571–1574
41. Huang S, Jiang Y, Li Z, Nishida N, Mathias P, Lin S, Ulvitch RI, Nemerow GR, Han J: Apoptosis signaling pathway in T cells is composed of ICE/Ced-3 family proteases and MAP kinase kinase 6b. Immunity 1997, 6:739–749
42. Kothakota S, Azuma T, Reinhard C, Klippel A, Tang J, Chu K, McGarry TJ, Kirschner MW, Koths K, Kwiatkowski DJ, Williams LT: Caspase-3-generated fragment of gelsolin: effector of morphological change in apoptosis. Science 1997, 278:294–298
43. Feinstein E, Kimchi A, Wallach D, Boldin M, Varfolomeev E: The death domain: a module shared by proteins with diverse cellular function. Trends Biochem Sci 1995, 20:342–344
44. Van Parijs L, Ibraghimov A, Abbas AK: The roles of costimulation and Fas in T cell apoptosis and peripheral tolerance. Immunity 1996, 4:321–328
45. Hamad AR, Schneck JP: Antigen-induced T cell death is regulated by CD4 expression. Int Rev Immunol 2001, 20:535–546
46. Ishimaru N, Yanagi K, Ogawa K, Suda T, Saito I, Hayashi Y: Possible role of organ-specific autoantigen for Fas Ligand-mediated activation induced cell death in murine Sjögren's syndrome. J Immunol 2001, 167:6031–6037

Available online at www.sciencedirect.com

SCIENCE DIRECT

Autoimmunity Reviews 4 (2005) 479–484

AUTOIMMUNITY REVIEWS

www.elsevier.com/locate/autrev

The possible etiopathogenic genes of Sjögren's syndrome

Masami Takei[a,1], Hidetaka Shiraiwa[a,1], Takashi Azuma[b], Yoshio Hayashi[c], Naoyuki Seki[d], Shigemasa Sawada[a,e,*]

[a]*Department of Internal Medicine, Division of Hematology and Rheumatology, Nihon University, School of Medicine, Tokyo, Japan*
[b]*Department of Internal Medicine, Saitama Hospital, Saitama, Japan*
[c]*Department of Pathology, Tokushima University School of Dentistry, Tokushima, Japan*
[d]*Department of Clinical Molecular Biology, Graduate School of Medicine, Chiba University, Chiba, Japan*
[e]*Department of Medicine, Nerima Hikarigaoka Hospital, Nihon University School of Medicine, 2-11-1 Hikarigaoka Nerima-ku, Tokyo, Japan*

Received 17 April 2005; accepted 10 May 2005
Available online 31 May 2005

Abstract

Sjögren's syndrome is a chronic autoimmune disease characterized by focal lymphocytic infiltration of lacrimal and salivary glands, but the precise mechanism of this syndrome is unclear. To clarify the pathogenesis of Sjögren's syndrome, the related genes must be identified. In the present study, we investigate the increased expression of genes and molecules related to Sjögren's syndrome and present our findings of cDNA microarray analysis in the mouse model. Furthermore, we present the results of immunohistochemical analysis of salivary glands in the mouse model and patients with Sjögren's syndrome. This approach might open a new discussion of the existence of principal pathogenic molecules in Sjögren's syndrome.

Keywords: Sjögren's syndrome; MRL/lpr mice; NFS/sld mice; cDNA microarray; Human homologue of SS related genes

Contents

* Corresponding author. Department of Medicine, Nerima Hikarigaoka Hospital, Nihon University School of Medicine, 2-11-1 Hikarigaoka Nerima-Ku, Tokyo, Japan. Tel.: +81 3 3979 3611; fax: +81 3 3979 3868.
E-mail address: sswd98@med.nihon-u.ac.jp (S. Sawada).
[1] First two authors equally contributed.

1568-9972/$ - see front matter © 2005 Elsevier B.V. All rights reserved.
doi:10.1016/j.autrev.2005.05.003

1. Mouse model of Sjögren's syndrome

Sjögren's syndrome (SS) is an autoimmune disease characterized by the massive infiltration of lymphocytes into exocrine glands, such as salivary and lacrimal glands, and the subsequent destruction of these exocrine glands. Like other autoimmune diseases, the etiology of SS remains unclear, but previous studies suggest the involvement of hereditary and environmental factors in the onset and progression of the disease. The disease is usually benign and many patients live a typical lifespan. However, the most common symptoms, dry eyes and dry mouth, are problematic and deeply influence patients' quality of life. In addition to these relatively benign manifestations, abnormalities of more vital organs such as renal tubular acidosis, interstitial pulmonary fibrosis, and central nervous system involvement have been demonstrated [1–4]. Therefore, it is important to determine the etiology of SS for the improved management of the disease.

An animal model is one of the most useful tools for studying the pathogenesis of SS; several mouse models have been generated and extensively studied. Among these models, the MRL/lpr mouse bearing the *lpr* gene with a deletion of Fas antigen spontaneously develops systemic vasculitis, glomerulonephritis, arthritis, and sialoadenitis. High levels of autoantibodies, immune complexes, and rheumatoid factor have also been observed in this mouse model [5,6]. Inflammation of the salivary glands in the MRL/lpr mouse is widely accepted as a pathogenic model for human secondary SS [7]. Although the fundamental molecular abnormality in the MRL/lpr mouse model directly depends on the *lpr* gene, the extent of the phenotype and the timing of onset are strongly influenced by background genes [8–10].

The NFS/sld mutant mouse is an animal model of primary SS that bears an autosomal recessive gene that arrests sublingual gland differentiation. Autoimmune sialoadenitis develops when NFS/sld mice undergo a thymectomy 3 days after birth without any immunization (Tx-NFS/sld mice). While no significant inflammatory lesions are observed in other organs or in NFS/sld mice that do not undergo a thymectomy (non-Tx-NFS/sld mice), significant inflammatory changes occur in the salivary glands of Tx-NFS/sld mice 4 weeks after their thymectomy [11,12].

2. cDNA Microarray analysis

Gene expression analysis provides an important perspective on unknown biological phenomena. The following methods are established and applied for basic and clinical studies: differential display [13], suppression subtractive hybridization [14], cDNA microarray hybridization [15], and serial analysis of gene expression (SAGE) [16]. A microarray system is a powerful tool for analyzing the expression profile of thousands of genes in a wide range of biological systems. Recently, microarray analysis has been applied for the research of various clinical disorders such as lymphoma, Huntington's disease, and myocardial infarction, and disease-related genes were isolated in some of these disorders [17–21].

In the present study, we isolated genes that contribute to the progression of SS, using mRNA from SS model mouse salivary glands and an in-house cDNA microarray, and identified up-regulated genes.

3. Sjögren's syndrome-related genes and molecules

To investigate the gene expression profile in SS, we examined the mRNAs of the MRL/lpr and NFS/sld mouse salivary glands using cDNA microarrays. We arrayed a set of 4608 cDNA clones derived from oligo-capped mouse brain, fetus, kidney, and spleen. The most aggressive inflammation in the salivary gland of MRL/lpr mouse occurs at the age of 12–16 weeks [8,22], so we compared the mRNAs of MRL/lpr and MRL/++ mouse salivary glands at the age of 16 weeks. We identified 15 highly expressed genes [*IL-16*, *Grap*, *caspase3*, *Ly-6C.2*, *Mel-14 antigen*, *cathepsin B*, *mpt1*, *Laptm5*, *Gnai2*, *vimentin*, *UCP2*, *saposin*, *Trt*, *laminin receptor 1*, *and HSP 70 cognate*] in the salivary gland of MRL/lpr mouse by cDNA microarray analysis, which were likely to be SS-related genes [23] (Table 1).

We performed reverse transcription-polymerase chain reaction amplification to confirm the high expression of the following 15 genes. High expression was verified in 11 of the 15 genes: *IL-16*, *Grap*, *caspase3*, *Ly-6C.2*, *vimentin*, *Mel-14 antigen*, *cathepsin B*, *mpt1*, *Laptm5*, *Gnai2*, and *UCP2*. Five of these genes (*caspase 3*, *Ly-6C*, *vimentin*, *Mel-14 antigen*, and *cathepsin B*) have already been recognized in patients with SS or the SS mouse model [24–29].

Table 1
Highly expressed genes in MRL/lpr mice salivary gland in comparison with MRL/++

Accession No.	Name of genes	Fold change[a]
NM_009810	Mus musculus *caspase 3*	2.31
M18466	Mouse lymphocyte differentiation antigen *Ly-6C.2*	2.75
M26251	Mouse *vimentin*	2.21
M25324	Mouse peripheral lymph node-specific homing receptor (*MEL-14* antigen)	3.50
NM_007798	Mus musculus *cathepsin B*	1.84
AF006467	Mus musculus membrane-associated phosphatidylinositol transfer protein (*mptl*)	1.98
NM_010686	Mus musculus lysosomal-associated protein transmembrane 5 (*Laptm5*)	2.16
NM_008138	Mus musculus guanine nucleotide binding protein, alpha inhibiting 2 (*Gnai2*)	1.93
U69135	Mus musculus *UCP2*	2.06
S36200	Mouse saposin=sphingolipid activator protein	1.88
NM_009429	Mus musculus translationally regurated transcript (*Trt*)	1.82
NM_011029	Mus musculus laminin receptor 1 (*Lamr1*)	2.02
M19141	Mouse heat shock protein 70 cognate	1.61
AF175292	Mus musculus neuronal *IL-16*	2.20
NM_027817	GRB2-related adaptor protein (*Grap*), mRNA	1.85

[a] The averages of the fold change based on the normalized microarray fluorescent data of MRL/lpr compared to MRL/++ ($n=8$).

Although a high expression of *caspase 3* has been reported in the NOD mouse model of SS [24], the MRL/lpr mouse is Fas-deficient and thus lacks Fas/Fas ligand pathway-dependent apoptosis. This suggests that Fas/Fas ligand pathway-independent apoptosis, such as perforin-or granzyme-dependent apoptosis [30], is induced in MRL/lpr mouse salivary glands. One of the adaptor molecules, Grap, effectively delivers signals from the immune cell surface to a downstream functional molecule. Grap has a structural arrangement of an SH3-SH2-SH3 domain, which is similar to that of other immune cell adaptor molecules such as Grb2, Gads, and Grap2 [31]. Grap is known to be specifically expressed in lymphoid tissues, and structurally resembles Grb2 more than other Grb2 family molecules in that Grap does not have the proline-rich motif. By immune cell activation, Grap binds to phosphorylated tyrosine of the local area transport (LAT) at its SH2 region, and further binds to Son of sevenless (Sos) in a manner similar to that of Grb2. Further down-stream events remain unknown. We have observed that the expression of Grap in the salivary glands of the model mice was higher than that of the control mice. Furthermore, we have identified 7 genes in the spleen of MRL/lpr mice not found in the spleen of MRL/+ mice using the mouse spleen cDNA microarray chip [32] (Table 2). Namely, the *Grap* gene was commonly up-regulated in the spleen and salivary glands from MRL/lpr mice [32]. Immunohistochemical staining in the salivary gland revealed substantial differences between MRL/lpr and MRL/++ in the expression of mouse Grap. Furthermore, the immunohistochemical staining of specimens from 3 patients with SS and 2 controls (subjects with salivary cysts) indicated that the human homologue of Grap was expressed on ductal cells and on certain infiltrating cells in patients with SS, but very weakly in the controls [32]. These results may suggest that in diseased salivary glands and spleen, enhanced stimulation of T cell receptor augments signal transduction to downstream molecules associated with apoptosis. Further detailed analysis of the Grb2 family may clarify the regulation of T cell differentiation and apoptosis in SS.

Table 2
Highly expressed genes in MRL/lpr mice spleen in comparison with MRL/++

Accession No.	Name of genes	Fold change[a]
U88682	Mouse anti-DNA antibody heavy chain variable region mRNA	2.88
XM_134565	Mouse similar to Gag-Pol polyprotein mRNA	1.93
M16072	Mouse Ig active gamma-2a H-chain V-Dsp2.2-J2-C mRNA	1.64
BC036286	Mouse myeloid/lymphoid or mixed-lineage leukemia 5, mRNA	2.17
NM_025408	Mouse phytoceramidase, alkaline (Phca)mRNA	3.23
X76772	Mouse mRNA for ribosomal protein S3	1.56
NM_027817	Mus musculus GRB2-related adaptor protein (*Grap*), mRNA	2.82

[a] The averages of the fold change based on the normalized microarray fluorescent data of MRL/lpr compared with MRL/+ ($n=6$).